1971

Slab behavior of a prestressed concrete box-beam bridge -- hazleton bridge, February 1971

Anton W. Wegmuller

Gerardo C. Cordoba

David A. VanHorn

OFFICE
OF
RESEARCH

LEHIGH UNIVERSITY

Prestressed Concrete Box-Beam Bridges

Progress Report No. 10

SLAB BEHAVIOR OF A PRESTRESSED CONCRETE BOX-BEAM BRIDGE

HAZLETON BRIDGE

by
Anton W. Wegmuller
Gerardo C. Cordoba
David A. VanHorn

Fritz Engineering Laboratory Report No. 315A.2

COMMONWEALTH OF PENNSYLVANIA

Department of Transportation

Bureau of Materials, Testing and Research

Leo D. Sandvig - Director
Wade L. Gramling - Research Engineer
Kenneth Heilman - Research Coordinator

Project No. 68-27: Structural Response of Prestressed Concrete Box-Beam Bridges

SLAB BEHAVIOR
of a
PRESTRESSED CONCRETE BOX-BEAM BRIDGE
HAZLETON BRIDGE

by

Anton W. Wegmuller
Gerardo C. Cordoba
David A. VanHorn

This work was sponsored by the Pennsylvania Department of Transportation; U. S. Department of Transportation, Federal Highway Administration; and the Reinforced Concrete Research Council. The opinions, findings, and conclusions expressed in this publication are those of the authors, and not necessarily those of the sponsors.

LEHIGH UNIVERSITY

Office of Research

Bethlehem, Pennsylvania

February, 1971

Fritz Engineering Laboratory Report No. 315A.2

TABLE OF CONTENTS

ABSTRACT

This report describes part of the field testing of a beam-slab type highway bridge constructed with prestressed concrete box girders, and subjected to loading with a test vehicle approximating AASHO HS 20-44 loading. The overall investigation includes studies of the behavior of the slab, and of lateral distribution of the vehicle loading. The purpose of this report is to describe the experimental investigation performed on the bridge slab.

The testing consisted of the continuous recording of slab surface strains at various locations as the test vehicle was driven over the span at various speeds. Investigations are included on the lateral distribution of strains and stresses in the slab, the effect of speed on stresses, and local wheel load effects. Finally, a comparison of moments obtained experimentally with the design moment specified by AASHO is given.

1. INTRODUCTION

1.1 Object and Scope

The purpose of this investigation was to develop information on the magnitude of slab strains produced by live loads in a beam-slab type box-girder bridge, located near Hazleton, Pennsylvania. The test structure was a multi-span simply supported bridge, with a cast-in-place concrete slab supported by five prestressed, precast box-beams laterally spaced at 9 feet 6 inches. The test span was 71 feet 1 inch in length.

Due to the interaction of the beams and slab, the evaluation of stresses in the slab is a difficult analytical problem. As a result, many authors attempted to solve the problem of lateral distribution of load analytically. However, most currently used methods of analysis do not account for many variables involved in the structural behavior of the beam-slab assemblage, and none is thoroughly verified by test results.

The need for an experimental verification of the lateral distribution of vehicular loads led to the initiation of a research project at Lehigh University in 1964. The primary purpose was to experimentally determine the actual lateral distribution of vehicular live loads to the stringers of the spread box-beam type superstructure. In a later step it was decided to investigate the behavior of the slab for the same bridge type.

In the phase of investigation reported herein, strains at different locations in the slab of a prestressed concrete

highway bridge were measured. Strain data was obtained from gages located at two slab panels instrumented at the section of maximum moment and from gages applied at a panel located at quarter span. The data gathered allowed the computation of stresses and bending moments at different locations of the slab panels investigated. The field testing was conducted with the Federal Highway Administration field test unit, consisting of a loading truck and monitoring trailer. Test runs across the bridge were made by directing the truck along several loading lanes, spaced across the width of the bridge deck. It is the purpose of this report to present and interpret the experimental results.

1.2 Previous Research

An exact analysis of the slab of a beam-slab type highway bridge is recognized as a difficult problem. Several theories have been developed to predict the behavior of the slab, or at least to give an economical and fast method of design. However, none of the theories accounts for all variables governing the structural behavior. A recent literature survey and review of existing methods of slab analysis and design of highway girder bridges is given in Ref. 3. The state of the art of current slab design is also summarized in Ref. 13.

The present AASHO (1969) Specifications for Highway

Bridges are primarily based on theoretical work done by Westergaard[12] and Newmark[9]. These standards lead to a rapid design of the slab, but fail to allow for many important variables associated with the behavior of slabs, such as torsional stiffness of the beams, varying thickness of the slab, and the restraint between beams and slab. Pigeaud[3] provided a series of charts to determine the longitudinal and transverse bending moments caused by live loads in the slab. However, this method does not account for the continuity of the slab over several girders.

Early experimental investigations to determine the effective width of slabs acted upon by wheel loads were made by Kelley[14] and Newmark[9,11]. Kelley[14] also provided interesting contributions to slab design, but as in Pigeaud's work, the effects of the continuity of the slab and of the torsional stiffness of beams were not included. As mentioned above, the paper by Westergaard[12] and the introduction of Westergaard's Modified Formulas, developed by Erps, Googins and Parker[10], provided the basis for the current AASHO[2] specifications governing slab design. These modified formulas for computing slab bending moments permit the inclusion of various end-fixities using appropriate factors ranging from 0.5 to 1.0. These factors are assigned according to the type of beam and the degree of composite connection between beam and slab.

At Lehigh University, the problem of load distribution

in spread box-beam bridges has been under investigation since 1964. The studies were initiated by a pilot field test of the Drehersville bridge[4], and continued with field studies of the Berwick[5] and Brookville[6], White Haven[7] and Philadelphia bridges[8]. However, the first investigation concerning slab behavior was made on the Hazleton bridge, along with the investigation on lateral distribution of load which is described in detail in Ref. 15. The slab investigation performed on this bridge is the subject of this report.

2. TESTING

2.1 Test Bridge

The bridge studied in this report is located in Luzerne County, Pennsylvania, on Legislative Route 1009, and crosses over L.R. 170. The center span of this three span bridge, schematically shown in Fig. 1, was chosen as the test span. The bridge is simply supported and has a length of 69 feet 5 inches, center-to-center of bearings.

A cross-section of the bridge is shown in Fig. 2. The bridge consists of five identical precast prestressed box-girders, spaced at 9 feet 6 inches center-to-center. The girders are 48 inches wide and 42 inches deep. Specified were a minimum strength of f'_{ci} = 5000 psi for the prestressed concrete at the time of release, and a minimum 28-day strength of f'_c = 5500 psi.

The reinforced concrete slab, cast in-place over the girders, provides a roadway width of 40 feet and has a specified minimum thickness of 7-1/2 inches between beams (See Fig. 2). Actual measurements indicated that the slab thickness varies from 8.52 inches to 9.66 inches at the section of maximum moment and from 8.22 to 9.18 inches at the quarter-span section, as seen in Fig. 3. The girders and the slab were designed to carry the AASHO HS 20-44 Standard Truck Load. An 18-inch wide curb and a 15-inch wide parapet are provided along the edges of the roadway. Diaphragms of a thickness of 10 inches were cast

between beams at the center of the span, and of a thickness of 12 inches at the end supports.

2.2 Gage Sections and Locations

Two cross-sections of the bridge, Sections M and Q, as shown in Fig. 1, were selected for strain gage application. Section M was located 3.55 feet east of midspan, where the maximum test-vehicle moment was expected to occur as the drive axle passed over this section. Section Q was located 16.75 feet east of midspan, at approximately the quarter-span location.

To gather information on the lateral distribution of load to the girders, beams were gaged at the section of maximum moment only. A detailed description of the instrumentation used in this investigation on lateral distribution of load to the girders is given in Fritz Engineering Laboratory Report No. 315A.1[15].

For the slab study, gages were applied at Section M, as shown in Fig. 4, as well as at Section Q. As can be seen from this figure, three transverse slab gages were placed directly on the slab surface of each of the two slab panels tested at Section M. In addition, gages 13 and 27 were placed on transverse steel reinforcing bars. The figure also shows the location and designation of all strain gages mounted at Section Q. At this section, only one slab panel was instrumented. Gages 7, 21, and 32 were placed on transverse reinforcing steel bars, whereas transverse

gages 40, 42, and 44 were placed on the slab surface. Gages 39, 41, and 43 were provided to measure longitudinal strains. Due to a limited number of available recording channels, these seventeen gage locations were selected for the slab investigation.

2.3 Instrumentation

All gages used in this investigation were of the SR-4 electrical resistance type manufactured by the Baldwin-Lima-Hamilton Corporation. Each gage location was ground and sanded, followed by a thorough cleaning with acetone. The surface was then sealed with SR-4 cement. The gages on the top surface of the slab were then mounted and waterproofed for protection against the heavy traffic.

Strain data was recorded using the mobile instrument unit of the U. S. Bureau of Public Roads. The equipment was housed in a trailer, and consisted mainly of an oscillator, 48 gage circuit amplification channels, and three recording oscillographs. A detailed description of this instrumentation is given in Fritz Engineering Laboratory Report No. 315A.1[15].

2.4 Loading Lanes

Nine loading lanes were selected according to the lay-out shown in Fig. 2. (The circled numbers along the slab surface indicate the center of each of the loading lanes.) Lanes 1, 3, 5, and 7 coincided with the center-lines of the slab panels, whereas lanes 2, 4, and 6 were located on the center-lines of the

three interior beams. Lane 8 was located 21 inches south of the center-line of the bridge, and lane 9 was 11 feet 3 inches south of the bridge center-line. Lanes 8 and 9 were located on the roadway such that the wheels of the test vehicle moved along the center-line of a slab panel, and produced a maximum response at midspan of the slab.

2.5 Test Vehicle and Test Runs

The test vehicle used in this study was a three-axle diesel tractor semi-trailer combination which, when properly loaded with aggregate material, closely simulated an HS 20-44 design vehicle. The axle loads and dimensions of the test vehicle, and of the design load vehicle, are shown in Fig. 3.

A total of 118 runs at different speeds were conducted in the field testing of the Hazleton Bridge. For crawl runs, the truck was driven at a speed of 2 to 3 mph. A total of 28 crawl runs were conducted, along with some impact runs at a nominal speed of 10 mph. The remainder of the runs were speed runs with nominal speeds varying from 5 to 60 mph designed mainly to study the effect of speed on lateral distribution of load to the girders. Before and after several test runs, the gages were calibrated to relate the relationships of the oscillograph traces to base values. The time interval between subsequent calibrations was generally less than two hours, thereby assuring accurate measurement of strain.

2.6 Longitudinal Position and Timing

Vehicle position was indicated on oscillograph records through the use of air hoses placed transversely across the roadway in the path of the vehicle. These air hoses were placed at Section M, 40 feet east of Section M and 40 feet west of Section M. As each axle crossed an air hose, a pressure switch was actuated causing a sharp offset in a reference trace on the oscillograph records. These offsets were in turn used to correlate the truck position with strain values recorded on the oscillograph records. Two additional hoses on each side of Section M were used to determine vehicle speed during speed runs. These hoses served to actuate a digital timing device, which enable rapid computation of average vehicle speed across the span.

3. DATA REDUCTION AND EVALUATION

3.1 Oscillograph Reading

Data reduction began with the identification of traces for each test run. This identification required the correlation of trace numbers and strain gages with the traces on the test record. After editing, calibration records were evaluated. Calibration of the galvanometers was required periodically during testing to ensure accurate strain measurement. A detailed description of the calibration procedure is given in previous reports[4,5,6,7,8,15] in the investigation on lateral distribution of load to the girders of the spread box-beam bridges.

Following editing and determination of calibration values, the records of all test runs were processed. The vertical excursion of each oscillograph trace from its original position at the start of the test run is a measure of the strain produced by the applied live load. These excursions were taken from corresponding traces, and hence slab surface strains at the location of the gages could be computed. In all cases, the maximum amplitude was located by eye. Typical traces for a crawl and a speed run are shown in Fig. 5. A smooth trace is characteristic of all crawl runs, whereas speed runs typically produced an oscillating response.

3.2 Evaluation of Oscillograph Data

3.2.1 Transverse Strains

Traces from the slab gages show a characteristic peak in response which is not present for gages placed on beams. A typical oscillograph trace for a slab gage is shown in Fig. 5. Due to the presence of local effects caused by concentrated wheel loads, two characteristic vertical excursions could be measured from each trace representing a particular run, namely, vertical excursions V(1) and V(2), together with corresponding calibration offsets. V(1) represents the probable (and assumed) excursion that would have been read if there had not been a local effect caused by concentrated wheel loads, and V(2) represents the actually recorded overall excursion including these local effects. The two separate excursions were evident only if a wheel passed directly over the gage or near the gage under consideration.

These trace amplitudes were entered as input in a first computer program, written in FORTRAN IV, which was set up to compute transverse strains $\epsilon_x(1)$ based on V(1) and $\epsilon_x(2)$ based on V(2), occuring in the slab of the tested bridge. This conversion of vertical excursions (oscillograph trace amplitudes) to strain values, involved a multiplication of the trace amplitude measured, by several parameters which were dependent on the electrical circuit for a particular gage. Hence, gage constants

(consisting of gage resistance, gage factors, cable length, operation attenuation, and calibration attenuation), calibration values, and vertical excursions served as program input. The program output, consisting of data input for verification and computed strains $\epsilon_x(1)$ and $\epsilon_x(2)$ was listed separately for each gage and test run, thus providing a clean and permanent record. At the same time, the computer was instructed to punch this information on data cards for convenient use as input for subsequent computation of stresses and moments, as described in the following sections.

3.2.2 Longitudinal Strains

As described in the report on lateral distribution of load for the Hazleton bridge[15], a computer program was developed to calculate the location of the neutral axis at each girder face, using measured beam strains. The cited report describes this program in detail, along with the applied statistical approach for rejection of inaccurate strain values. For the slab investigation, using beam strain data, the program could conveniently be used to extrapolate (at all locations of interest) the longitudinal strains occuring in the slab. A linear distribution of strain extending from the beam faces into the slab was assumed for this step. However, no beam strains were recorded at the quarter span section (Section Q), and therefore a different approach had to be taken. As illustrated in Fig. 6, it was

assumed that for a given girder face and test run the location of the neutral axis at the quarter span section was the same as the location of the neutral axis at the section of maximum moment. Then, using longitudinal strains measured at the beam-slab interfaces, it was possible to extrapolate longitudinal strains at desired locations.

Similarly, no longitudinal strains were measured at the center of the slab panels at Section M. Therefore, these longitudinal strains were found by linear interpolation of corresponding computed longitudinal strains near the junctures of beams and slab.

3.2.3 Slab Bending Stresses

Knowing transverse strains ϵ_x and longitudinal strains ϵ_y at a given point, transverse stresses σ_x and longitudinal stresses σ_y could be computed. A second computer program was developed to calculate these stresses in the slab at all locations of transverse slab gages, shown in Fig. 4. Theory of elasticity[1] yields, for a two-dimensional state of stress:

$$\sigma_x = \frac{E}{1-\nu^2}[\epsilon_x + \nu\,\epsilon_y] = 1.033\,E[\epsilon_x + \nu\,\epsilon_y]$$

$$\sigma_y = \frac{E}{1-\nu^2}[\epsilon_y + \nu\,\epsilon_x] = 1.033\,E[\epsilon_y + \nu\,\epsilon_x]$$

Where: E = Modulus of elasticity of slab concrete

ν = Poisson's Ratio (taken as 0.18)

ϵ_x = Measured strain in transverse direction

ϵ_y = Measured strain in longitudinal direction

σ_x = Computed stress in transverse direction

σ_y = Computed stress in longitudinal direction

An assumed value of $E = 5000$ ksi was used to compute transverse stresses $\sigma_x(1)$ based on first trace amplitude, transverse stresses $\sigma_x(2)$ based on second excursion, as well as longitudinal stresses σ_y. The program output, consisting of data input and computed stresses, as well as the run information, was again listed separately for each gage and run. However, no principal stresses could be computed since strains in only two directions had been measured.

3.2.4 Slab Bending Moments

In a last step of this investigation, bending moments based on curvatures produced in the slab due to wheel loads were evaluated. This could be done only at sections where transverse slab gages were mounted on top as well as on bottom fibers of the slab. Bending moments due to transverse stresses only could be computed. This computation was based on a linear distribution of strain across the thickness of the slab. For a homogeneous, elastic material, the expression for the bending moment in a plate is derived by Timoshenko[1], for example:

$$M_x = -D\left[\Phi_x + \nu\,\Phi_y\right] = -\frac{E\,h^3}{12(1-\nu^2)}\left[\frac{\partial^2 w}{\partial_x^{\,2}} + \nu\,\frac{\partial^2 w}{\partial_y^{\,2}}\right]$$

Where: M_x = Moment due to transverse stresses (ft. lb./ft.)

D = Plate bending stiffness

h = Effective thickness of slab

Φ_x = Curvature of the slab in transverse direction

Φ_y = Curvature of the slab in longitudinal direction

In order to apply the above expression, the slab was assumed to be a homogeneous, elastic material, and the slab reinforcement was neglected. The effect of the curvature Φ_y was neglected since its value is small and in addition is multiplied by Poisson's Ratio (taken as 0.18), making the second term in the parenthesis much smaller than the first. Having evaluated transverse strains at top and bottom fibers of the slab cross-section, the curvatures Φ_x could be readily computed. To compute transverse slab bending moments from measured strains, an average value of E = 5000 ksi for the modulus of elasticity of the slab concrete was again assumed, since there is no way of determining the actual value of E from field tests. An additional subroutine was written to compute the transverse slab bending moments based on the first vertical excursion. The computed moments were then compared with design values.

4. PRESENTATION OF TEST RESULTS

4.1 Maximum Measured Slab Strains

Maximum measured transverse compressive and tensile strains occurring at each gage location, and considering all runs, are compiled in Table I. These maximum values are given separately for crawl runs and for speed runs, both for gages mounted on reinforcing steel bars and gages applied directly on the slab surface. Separate values are given for strains based on first and second excursions.

Table I shows that for crawl runs as well as for speed runs, the maximum measured tensile strain was 28.8 μ in/in for gages mounted on the reinforcing steel bars, when neglecting local effects. Including local effects due to concentrated wheel loads, a maximum tensile strain of 100.5 μ in/in was recorded. For gages placed on the concrete surface the maximum measured tensile strain was 72.5 μ in/in. From the magnitude of the measured tensile strains it can be concluded that the slab section was probably never cracked. This justifies the assumption of a homogeneous material for the computation of stresses and moments in the slab.

Maximum measured compressive strains, considering all gage locations, were 61.7 μ in/in when neglecting local effects and 76.6 μ in/in considering local effects. Most longitudinal strains were found to be small and compressive, but a maximum

tensile strain of 60.0 μ in/in was also recorded.

Generally, maximum strain values were found to be small, and with a few exceptions, strains were slightly greater for speed runs than for crawl runs. In all tables and figures, a positive sign indicates compression and a negative sign tension at a particular location.

4.2 Maximum Slab Stresses

Maximum computed transverse compressive and tensile stresses occurring at the gage locations investigated, are given in Table II. These maximum values of stresses are given separately for crawl and speed runs, and based on first and second vertical excursions. All runs were considered in this compilation.

Table II shows that for crawl runs as well as for speed runs, the computed maximum transverse tensile stress was 277 psi when neglecting local effects. Considering local effects, tensile stresses up to 384 psi were found; thus indicating that the slab was probably never cracked. Maximum computed transverse and longitudinal compressive concrete stresses were found to be far below allowable stresses. However, it should be noted that the actual pavement thicknesses (See Fig. 4 a) are consistently greater than the minimum thicknesses specified on the design drawings (See Fig. 2).

4.3 Influence Lines for Strains and Stresses

In Figs. 8 through 16, influence lines for transverse

strains and stresses occurring at different gage locations are presented, to show the variation of strain and stress for different load positions. Experimentally determined strains $\epsilon_x(1)$, neglecting local effects and $\epsilon_x(2)$, considering local effects are plotted for a truck centered in each loading lane. The graphs contain the information gathered from all crawl runs and are based on average values computed from three to four runs. Inspecting the influence lines for strains $\epsilon_x(2)$ reveals a similarity in shape with influence lines based on strains $\epsilon_x(1)$ with the exception of a region affected by local strains caused by concentrated wheel loads. In this region, a considerable deviation can be recognized indicating the heavy influence of these local effects. Figs. 17 through 19 show some influence lines for longitudinal strain and stress.

The same figures also illustrate the lateral variation of transverse stresses for different load positions. Since the modulus of elasticity of the slab concrete is unknown, it was decided to present combined strains $(\epsilon_x + \nu \epsilon_y)$ rather than actual stresses. If values of stresses in (psi) are desired, each given combined strain value must be multiplied by $E/(1-\nu^2)$, where E is to be taken in (psi). Hence, the reader may exercise his individual judgment in estimating a value for E in order to arrive at stresses. Again, all influence lines are based on the information compiled from crawl runs only and average values are shown for each gage. The graphs separately show combined strains neglecting local effects and combined strains considering local effects due

to concentrated wheel loads. Since the behavior of the structure for positions of the load other than centered in loading lanes is unknown, a straight line interpolation was used between adjacent loading lanes. Lane location, gage number and location are indicated in each plot.

4.4 Variation of Strain and Stress Across Slab Thickness

The measured values of strain indicate that the slab sections probably were never cracked. This conclusion is based on the fact that all measured strains were considerably smaller than the strains obtained from a cracked section analysis. Hence, a linear variation of strain was assumed across the slab thickness.

Figs. 20 through 24 show influence lines for transverse strain for pairs of top and corresponding bottom gage. The purpose of these diagrams is to show the variation of transverse strain across the slab thickness. A variation in the location of the neutral axis in the slab for different truck positions can be recognized as well as the occurrence of in-plane (membrane) strains. This strain variation is presented for five different sections. Once again, gage numbers and locations as well as lane numbers are shown in the plots. Similar influence lines for longitudinal strains are shown in Figs. 25 and 26, and Figs. 27 and 28 show longitudinal stresses at the same gage locations.

4.5 Influence Lines for Transverse Slab Moments

Figs. 29 through 33 show the variation of transverse

slab bending moments for different truck positions, computed at the sections indicated in Fig. 7. For this presentation, the modulus of elasticity of the slab concrete was taken as E = 5000 ksi and a Poisson's Ratio of $\nu = 0.18$ was assumed. All given values are based on information collected from crawl runs, and average values computed from three to four runs are shown. The influence line shown in each figure depicts the transverse slab moment M(l) based on stresses, neglecting local effects. A linear distribution of strains across the slab thickness was assumed for the computation of moments. The implementation of this assumption is discussed in a later section of this report.

Such influence lines may be used to advantage by the designer to find maximum values of bending moments produced by trucks moving simultaneously along different loading lanes. A superposition of moments, however, is only valid as long as the slab is uncracked.

4.6 Effect of Speed

As pointed out earlier, speed runs were mainly designed to study the effects of speed on the lateral distribution of load to the girders. During this investigation, it was found that the position of the wheel load with respect to the slab gage is of significant influence on the magnitude of strain produced at the location of the gage. Since only one run per lane and at each speed was conducted, no reliable average values could be computed. Therefore, it was not possible to study the effect of speed on

slab strains, stresses and moments in a conclusive manner.

To illustrate the variation in the test results, Figs. 35 through 38 depict the amplification factors versus speed for four different gages. The gages were chosen according to a load position for which the strain was expected to be maximum. A study of such diagrams did not reveal any definite dependency of strain on speed, and based on the present limited information, no conclusive results can be presented.

5. DISCUSSION OF TEST RESULTS

5.1 Maximum Strains and Stresses in the Slab

One of the main objectives in the testing of the slab of the Hazleton Bridge was the experimental measurement of the maximum strains and stresses caused by the moving truck load. A summary of maximum measured strains and computed stresses given in Tables I and II reveals that recorded strains and stresses were small. As will be shown, the design value for the slab bending moment prescribed by AASHO[2] was 3000 ft-lb/ft (See Sec. 5.5). Based on a homogeneous behavior of the slab, the design moment would cause slab stresses of ±320 psi for a solid, uncracked slab having a nominal thickness of 7-1/2 inches. Considering local effects, maximum measured transverse tensile stresses up to 390 psi were found, whereas, when neglecting local effects, transverse tensile stresses were below 230 psi. This indicates, that the pertrubation produced by wheel loads may create stresses which are several times larger in magnitude than the stresses based on the first trace amplitude.

A cracked-section analysis of the slab for the design moment (3000 ft-lb/ft) yields a compressive stress of 500 psi in the extreme concrete fiber and a maximum tensile stress of approximately 8800 psi in the reinforcing steel. A comparison of these computed values based on an assumed cracked section, with maximum measured values of stress and strain, leads to the following observations:

1. The applied live load probably never caused cracking in the slab. This statement is supported by the fact that measured maximum tensile strains in reinforcing steel bars were at most 100 μ in/in which is equivalent to a stress of approximately 3000 psi, which is far below the stress based on a cracked-section analysis.

2. All compressive stresses measured on the slab surface were lower than the computed cracked-section values.

5.2 Lateral Distribution of Strains

The influence lines shown for strains, stresses and moments clearly indicate the location of the truck for maximum positive or negative response at a slab section. In general, the load position producing maximum strain at the top of the slab was not the same that produced maximum strain at the bottom fibers of the slab. This fact reveals the presence of transverse in-plane (membrane) forces which cause a variation in the neutral axis location, depending on the position of the load.

For gages which were located at the center of the slab panels, the maximum stress was produced when the vehicle wheels passed the loading lane closest to this section. Gages located close to the face of the girders showed maximum response when one line of wheels was close to the gage and the other line of wheels was out of the slab span. In general, the gage response decreased as the test vehicle was run in lanes at greater lateral distance

from the section under consideration, eventually causing strains of opposite sign at this section. These strains could, in some cases, be as large as the strains produced when the load was near the gage under consideration.

Having analyzed the present information, it cannot be said with certainty whether the tested slab panels experience the maximum response in the slab. Similar tests on panels lying at different longitudinal positions, or a theoretical analysis, would answer this question. It is conceivable, although not necessarily probable, that panels located at other positions could be subject to more severe conditions.

5.3 Effect of Speed on Slab Strains

From the reduction of data, graphs of the type shown in Figs. 35 through 38 were obtained. As mentioned previously, a thorough investigation to study the effects of speed on slab strains, stresses and moments was not within the scope of these field tests. The relative position of the wheel loads with respect to the gage location is of greatest importance. However, it was possible only at crawl speed to accurately control the lateral position of the load vehicle. Hence, many runs conducted at the same speed would be needed to find reliable average values for strains. Although these graphs do not show a definite pattern for the variation of strain with speed, it is possible that higher speeds may produce higher stresses than those found for crawl speed.

5.4 Local Wheel Load Effect

Under the action of wheel loads, the slab deflects, producing curvatures in both transverse and longitudinal directions. The distribution of stresses in a slab acted upon by concentrated loads is difficult to determine analytically. This is due to the fact that near the area of application of load, a serious local perturbation of the present state of stress occurs. From the literature reviewed, it appears that no analytical solution for this complex three-dimensional problem exists.

Despite the fact that the phenomenon of local stresses caused by concentrated wheel loads was recognized long ago, it is still not well enough understood, and has not been experimentally investigated. One of the objectives of this investigation was to actually measure the magnification of stress due to the concentrated wheel loads.

From theoretical investigations on the corresponding two-dimensional problem we can conclude that the local stresses produced by concentrated wheel loads diminish rapidly across the thickness of the slab and with increasing distance from the area of application of load. Influence lines for strains plotted for a top and corresponding bottom gage reveal that the magnification of strains is always greater for gages located at top fibers of the slab. From the present investigation it was found that the ratio of transverse strains $\epsilon_x(2)/\epsilon_x(1)$ was mostly between 2 and 5, but could be as high as 10. It should be remembered that

these local stresses occur only over small areas near the points of application of load, and are therefore of a purely local nature. These additional stresses, produced by concentrated wheel loads, are compressive in nature and may even be redistributed due to possible local inelastic behavior of the slab concrete. The present limited information however, is not sufficient to establish possible detrimental effects, and more theoretical as well as experimental work is needed to improve the present knowledge.

5.5 Comparison of Design and Experimental Slab Moments

The AASHO[2] Standard Specifications for Highway Bridges prescribe the transverse slab bending moment produced by live load in a bridge slab panel by the formula:

$$M = \frac{(S + 2)}{32} P_{20}$$

Where: M = Transverse slab bending moment (ft-lb/ft)

S = Effective transverse span length of panel (in feet); i.e. clear span for slabs cast monolithically with beams

P_{20} = 16K = Half of the drive axle or rear axle load of the AASHO HS 20-44 Standard Truck

The Specifications also specify that the moment obtained by this formula should be multiplied by a factor of 0.8 for a

slab continuously spanning three or more supports. The longitudinal reinforcement should simply be designed by taking a specified percentage of the transverse slab reinforcement. For a clear span of 5.5 feet, the transverse bending moment for HS 20-44 truck loading (excluding impact, which is 30% for slabs) is found to be 3000 ft-lb/ft. According to the Specifications, this design moment value should be applied to both the positive midspan location as well as the negative moment locations at the supports. In practice, the slab is then designed as a rectangular section, using ordinary reinforced concrete procedures.

Figs. 29 through 33 show that the slab bending moments M(1), based on strains neglecting local effects, are nowhere larger than 3000 ft-lb/ft. Since the moment was computed based on a linear distribution of strain across the slab thickness, the validity of this assumption merits further discussion. For moment computations neglecting local effects, the assumption of a linear strain distribution across the slab thickness is reasonable. However, if local effects were to be included, this assumption would lead to only a rough approximation of the true moment occurring in the slab, since due to a three-dimensional state of stress caused by concentrated wheel loads, the distribution of strain across the slab thickness is non-linear. Hence, based on the stated assumption, the moments would be overestimated.

Assuming again a homogeneous uncracked behavior of the slab, the response of two trucks simultaneously crossing the

bridge and restricted to movement along prescribed loading lanes, was superimposed and compared with the response of a single truck. Table III shows either the maximum value of moment for superimposed truck responses or single truck response, whichever is larger. It is seen that superposition of the response of two trucks, generally does not lead to larger moments than found for single truck response. Hence, the present investigation shows that experimentally found moment values M(l) based on the first trace amplitude were smaller, in all cases, than design values based on AASHO[2] criteria. It is interesting to note that both of the experimentally determined maximum moments (negative and positive) in the slab occurred at Section C (See Table III and Fig. 7). This behavior is a reflection of the large torsional stiffness of the box-beams, and demonstrates that the displacement of the box-beams is primarily vertical, with very little rotation.

5.6 Slab Moments Predicted by Existing Theories

A summary of transverse slab bending moments as predicted by existing theories is given in Table IV. The basic parameters governing the structural behavior of the bridge slab are transverse slab span, geometry of slab, distribution of reinforcement, type of loading, support conditions, and area of application of load. A few of these theories will now be briefly described:

Kelley's[14] tests resulted in a series of empirical relationships predicting the effective width of a loaded slab panel.

Once this effective width is determined, the applied load is placed on the panel, with the width equal to the effective width, and the design of the slab can be made for a simple or fixed beam. Actually, the effective width depends on the type of loading, and the boundary conditions for the slab. Furthermore, the method does not account for different end restraints and the orthotropic nature of the slab. The experimentally derived relationships pertain to the slabs covered in Kelley's test program only, and an extrapolation to bridge slabs is not simple.

Westergaard[13] considered two types of slab, differing in the way in which they are primarily reinforced, namely:

Case I: Slabs with main reinforcement parallel to the direction of traffic, and

Case II: Slabs with main reinforcement perpendicular to the direction of traffic.

This distinction was made only to indicate the direction of the slab span and the position of the wheel loads. Homogeneous and isotropic material was assumed for his investigation and a circular area of application of load was chosen. Actually, the slab is orthotropic due to different amounts of reinforcement in longitudinal and transverse directions. Furthermore, the area of application of load is taken as rectangular and not circular. Also, the effect of the continuity of the slab is not accounted for.

In a later paper, Erps, Googins and Parker[10] simplified

Westergaard's original work. In addition, these authors introduced end-fixity factors to account for different end restraints. This investigation served as a basis for the current AASHO Specifications. Although the introduction of an end-fixity factor provides a step towards the correct solution, its estimation is a difficult task, since this factor depends on the geometry and the parameters governing the structural behavior of the entire bridge.

Newmark[9,11] presented analytical solutions for the bending moments occurring at different sections in the slab. This analysis is also based on a circular area of application of load and the effect of Poisson's Ratio was neglected. Again in this method, there was no consideration of the torsional stiffness of the stringers and no assessment of the restraint of the slab in the girders.

From the literature reviewed, it can be concluded that no rigorous method is presently available to analyze the slab of a beam-slab type highway girder bridge. Since the slab forms an integral part of the entire structure, it appears that the slab cannot be analyzed as a separate structural part, and thus its structural behavior can only be found by an overall analysis of the entire bridge structure.

6. SUMMARY AND CONCLUSIONS

6.1 Summary

The main objective of this report is to present and interpret the data collected in the field testing of the slab of a prestressed concrete box-beam bridge, located near Hazleton, Pennsylvania; to compare experimentally found stresses and moments with design values predicted by the AASHO Standard Specifications for Highway Bridges; and to study local effects caused by concentrated wheel loads. The slab investigation also served as a pilot study for future slab tests.

The field testing of the slab of the Hazleton Bridge, which consisted of five precast, prestressed concrete box-beams topped by a composite reinforced concrete slab, was conducted simultaneously with the main investigation on lateral distribution of load to the girders. Strain gages were applied to the slab surface and to some transverse reinforcing steel bars at two different sections of the bridge. These sections were located at quarter-span, and near midspan at a section where the maximum response in the girders was expected to occur when the drive axle of the truck passed over this section. One slab panel was instrumented at the quarter-span section, and two slab panels were gaged at the section of maximum moment. Additional gages, placed on girder faces, allowed an extrapolation of longitudinal strains produced in the slab.

Tests were conducted with the load vehicle moving either at crawl speed or at speeds varying from 5 to 60 mph. The truck was driven along nine different loading lanes. A mobile instrumentation unit, provided by the Federal Highway Administration, allowed the continuous recording of slab strains caused by the test vehicle. The data recorded in the field was reduced to strains, stresses, and bending moments. This reduction of data was done with the aid of a computer, and is described in detail in this report. Most of the data is presented graphically in the form of influence lines, reflecting the structural behavior of the slab.

A comparison of internal bending moments produced in the slab with those predicted by the AASHO Standard Specifications for Highway Bridges is presented, as well as a discussion of the local effects caused by concentrated wheel loads. Experimentally found values for slab bending moments (based on actual slab thickness and measured strains) compared with design moments predicted by the AASHO Specifications reveals that the experimental moments are generally smaller than the Specification values.

6.2 Conclusions

From the testing of the Hazleton Bridge, the following conclusions can be drawn:

1. Transverse and longitudinal strains and stresses measured at different gage locations on the slab surface

and on reinforcing steel bars were generally small, indicating an uncracked behavior of the slab.

2. Near the area of application of load, local stresses are produced in the slab which substantially increase the bending stresses. These additional stresses usually exceed the stresses computed from unaffected trace amplitudes. However, these local stresses, being compressive in nature, may be redistributed due to possible local inelastic behavior of the slab concrete. Based on the available limited information, it has not been established that those local stresses are detrimental in nature. Further theoretical and experimental investigations are needed, however, to more clearly establish the effects of these local stresses, and to enable their consideration in future slab design.

3. It is possible that strains and stresses are affected by speed. However, due to a lack of sufficient experimental data, no final conclusions can be drawn regarding the effect of speed on stress.

4. In general, the test structure responded predictably to lateral variation in load position. Maximum slab strains, stresses, and moments can be determined by making use of the influence lines presented in this report.

5. Experimentally found transverse bending moments, neglecting local effects were found to be smaller than design values prescribed by the AASHO Specifications.

6. Superposition of single truck response to determine the response of multiple trucks is valid only for an uncracked slab. For this bridge the superposition resulted in experimental slab bending moments which were generally less than the AASHO design value.

7. The findings from this investigation of slab behavior are the first reported in the current overall research investigation of beam-slab type bridge behavior conducted at Lehigh University. Therefore, at this time, the results will serve as a representation of the slab behavior at three different transverse slab spans in a typical spread box-beam superstructure. Similar results from the testing of two prestressed concrete I-beam bridges (Bartonsville and Lehighton) will form a basis for comparison of field test results, and will usefully provide a data base for the future analytical work required to develop possible revisions in specifications and procedures for deck slab design.

7. ACKNOWLEDGMENTS

This study was conducted in the Department of Civil Engineering and Fritz Engineering Laboratory, under the suspices of the Lehigh University Office of Research, as a part of a research investigation sponsored by the Pennsylvania Department of Transportation; the U. S. Department of Transportation, Federal Highway Administration; and the Reinforced Concrete Research Council.

The field test equipment was made available through Mr. C. F. Scheffey, now Director, Office of Research, Federal Highway Administration. The instrumentation of the test structure, and operation of the test equipment, were supervised by Messrs. R. F. Varney and H. Laatz, both from the Federal Highway Administration.

The basic research planning and administrative coordination in this investigation were in cooperation with the following individuals representing the Pennsylvania Department of Transportation: Mr. B. F. Kotalik, Bridge Engineer; Mr. H. P. Koretzky, and Mr. Hans Streibel, all from the Bridge Engineering Division; and Messrs. Leo D. Sandvig, Director; Wade L. Gramling, Research Engineer; and Foster C. Sankey and Kenneth L. Heilman, Research Coordinators; all from the Bureau of Materials, Testing, and Research.

The following members of the faculty and staff at

Lehigh University made major contributions in the conduct of the field tests and in the reduction and processing of the test data: Dr. C. N. Kostem, Prof. J. O. Liebig, Jr., Felix Barda, Cheng-Shung Lin, Yan-Liang Chen, Chiou-Horng Chen, Daryoush Motarjemi, and Donald Frederickson. The manuscript was typed by Mrs. Ruth Grimes, and the figures were prepared by John M. Gera and Mrs. Sharon Balogh.

8. TABLES

TABLE I(a): MAXIMUM MEASURED STRAINS ON REINFORCING STEEL BARS

Crawl Runs

Gage No.	13	27	7	21	32
Tensile Strain $\epsilon_x(1)$	-17.8	-25.6	-23.5	-24.2	-23.3
Tensile Strain $\epsilon_x(2)$	-47.8	-76.7	-44.5	-62.5	-100.5
Compressive Strain $\epsilon_x(1)$	3.6	6.3	13.5	6.1	2.0
Compressive Strain $\epsilon_x(2)$	3.6	6.4	21.1	6.2	3.3

Speed Runs

Gage No.	13	27	7	21	32
Tensile Strain $\epsilon_x(1)$	-3.9	-28.8	-18.1	-25.3	-0.8
Tensile Strain $\epsilon_x(2)$	-5.1	-32.1	-56.9	-34.4	-55.1
Compressive Strain $\epsilon_x(1)$	1.9	0.6	21.9	55.6	9.3
Compressive Strain $\epsilon_x(2)$	1.9	0.6	23.4	76.6	21.3

(Units of ϵ_x are μ in/in -
Stresses can be obtained as the product of the ϵ_x value and 29×10^6 psi)

TABLE I(b): MAXIMUM MEASURED STRAINS ON CONCRETE SLAB SURFACE

Crawl Runs

Gage No.	11	12	14	25	26	28	40	42	44
Tensile Strain ϵ_x(1)	-15.3	-6.2	-34.6	-46.0	-9.6	-23.9	-42.5	-6.6	-28.9
Tensile Strain ϵ_x(2)	-36.9	-6.2	-49.6	-56.3	-9.6	-29.9	-54.5	-72.5	-38.5
Compressive Strain ϵ_x(1)	11.6	16.1	---	28.1	20.6	20.8	19.5	13.3	16.2
Compressive Strain ϵ_x(2)	12.4	70.2	16.6	39.0	71.3	40.2	32.6	57.2	20.1

Speed Runs

Gage No.	11	12	14	25	26	28	40	42	44
Tensile Strain ϵ_x(1)	---	-5.8	-40.7	-37.3	-4.7	-28.0	-36.7	-4.3	-28.9
Tensile Strain ϵ_x(2)	---	-6.7	-41.5	-61.2	-7.3	-34.2	-65.8	-7.2	-40.5
Compressive Strain ϵ_x(1)	24.2	0.4	13.3	33.6	19.5	61.7	19.6	26.4	---
Compressive Strain ϵ_x(2)	44.2	0.8	16.9	44.2	29.7	72.9	42.5	32.6	---

(Units of ϵ_x are μ in/in -
Stresses can be obtained as the product of the ϵ_x value and 29 x 10^6 psi)

TABLE II: COMPUTED MAXIMUM STRESSES ON CONCRETE SLAB SURFACE

Crawl Runs

Gage No.	11	12	14	25	26	28	40	42	44
Tensile Stress $\sigma_x(1)$	-67	-24	-169	-227	-38	-114	-209	-27	-128
Tensile Stress $\sigma_x(2)$	-178	-24	-237	-281	-38	-152	-264	-384	-182
Compressive Stress $\sigma_x(1)$	76	104	---	153	128	120	113	74	93
Compressive Stress $\sigma_x(2)$	76	383	96	210	386	220	183	302	121
Compressive Stress σ_y	78	145	60	88	140	138	96	137	93

Speed Runs

Gage No.	11	12	14	25	26	28	40	42	44
Tensile Stress $\sigma_x(1)$	---	-20	-202	-182	-6	-136	-173	-11	-133
Tensile Stress $\sigma_x(2)$	---	-20	-205	-305	-21	-165	-338	-206	-201
Compressive Stress $\sigma_x(1)$	130	25	142	178	123	332	130	163	---
Compressive Stress $\sigma_x(2)$	234	25	142	240	176	390	235	206	---
Compressive Stress σ_y	77	116	96	181	154	126	131	248	133

(Units are psi - A value of 5×10^6 psi was used as the E for the concrete)

TABLE III: MAXIMUM TRANSVERSE MOMENTS

Section (See Fig. 7)	A	B	C	D	E
Max. (+) Moment M(l)	+1300	+1350	+3000	+1400	+1250
Max. (-) Moment M(l)	-400	-450	-2500	-400	-1100

(Units are ft-lb/ft)

TABLE IV: TRANSVERSE SLAB BENDING MOMENTS - COMPUTED BY EXISTING THEORIES OF SLAB ANALYSIS

Theory	At Center of Slab Panel	At Supports of Slab Panel	Remarks
AASHO	3000	-3000	
Westergaard (original)	3800	----	Based on 75% End Restraint
Westergaard (modified)	3710	----	Based on 75% End Restraint
Kelley	4200	----	
Newmark	4470	----	

(Units are ft-lb/ft)

9. FIGURES

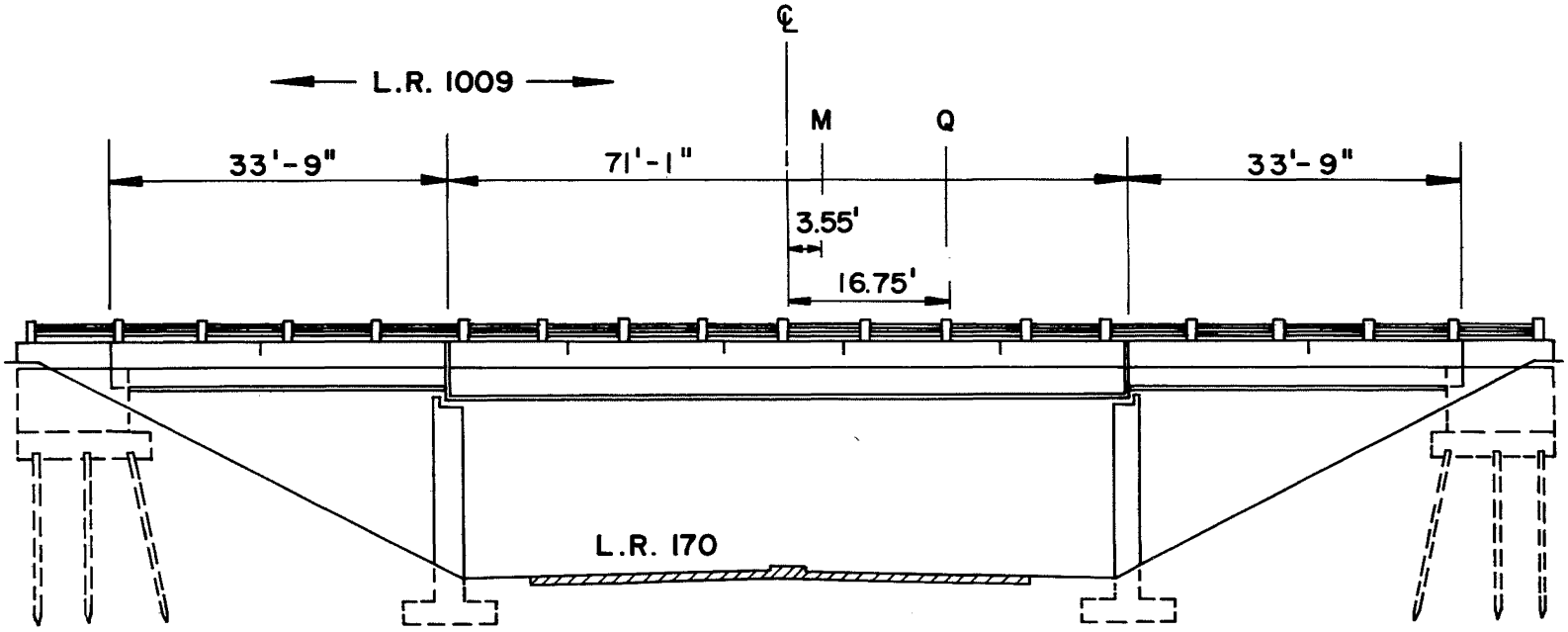

M- Section of Maximum LL Moment
Q- Section at Quarter Span

Fig. 1 Elevation of Test Bridge

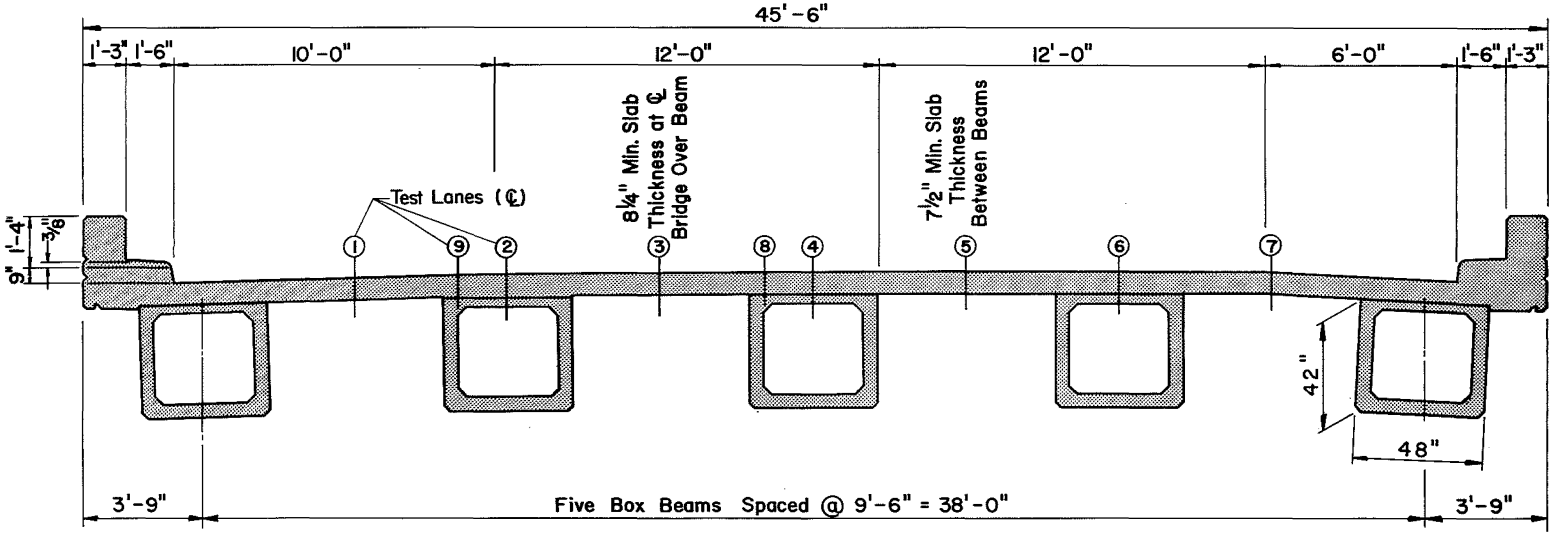

Fig. 2 Cross Section of Box-Beam Bridge

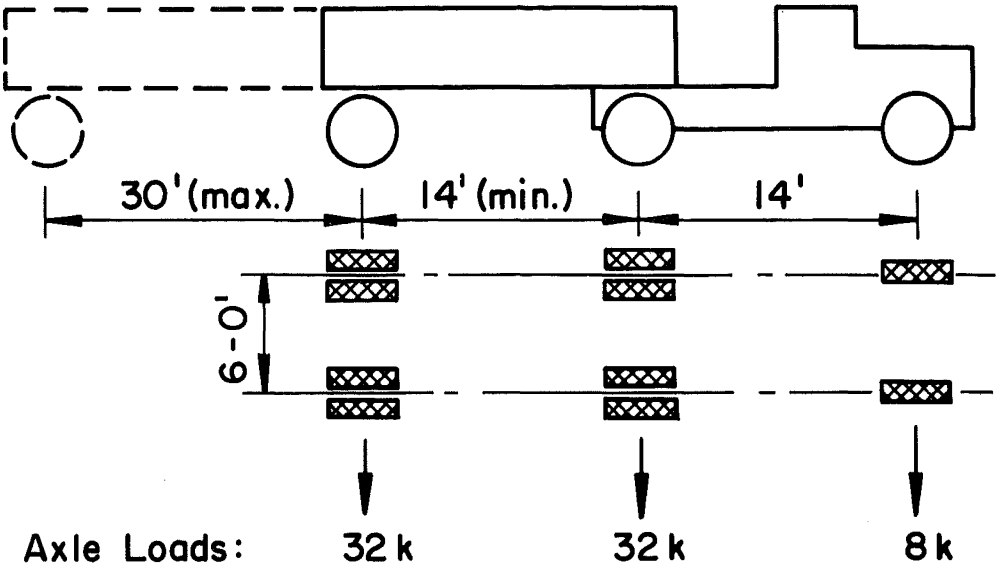

HS 20-44 Design Load Vehicle

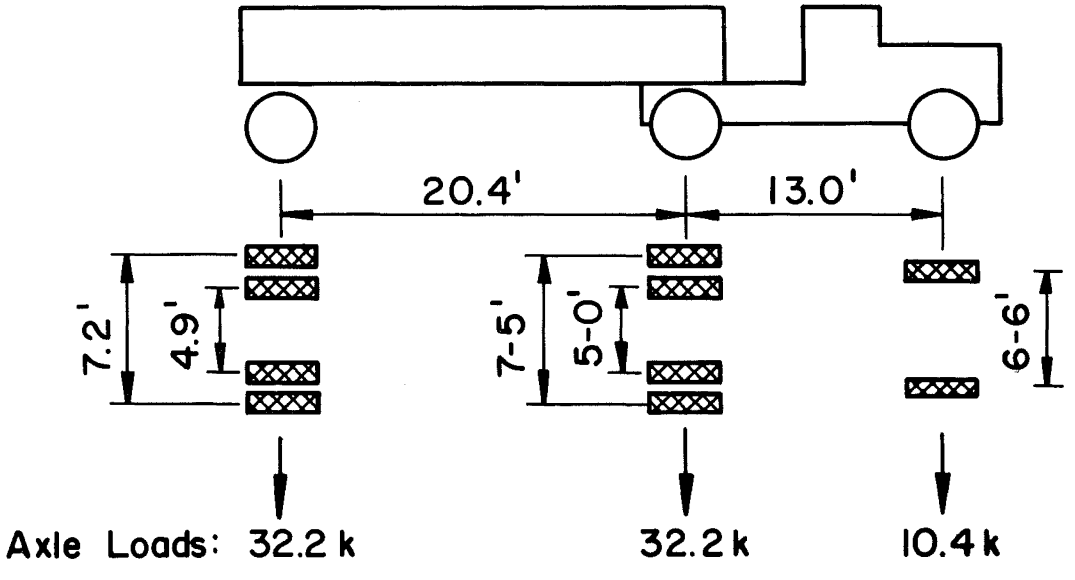

Test Vehicle

Fig. 3 Characteristics of Design and Test Vehicles

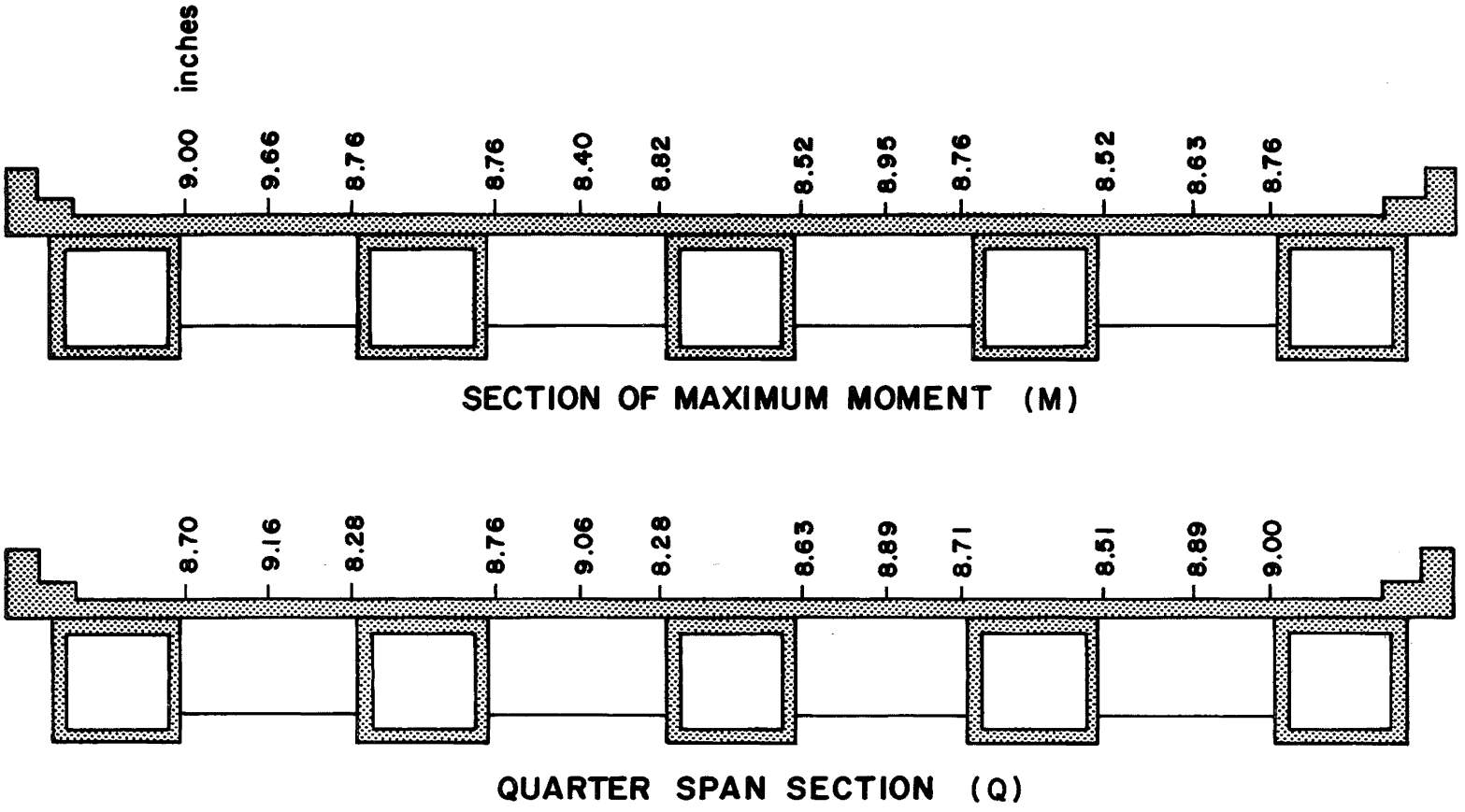

Fig. 4a Measured Slab Thickness

HAZLETON BRIDGE

Span : 69'-7"
Beam Spacing : 9'-6"
Beam Size : 4' x 42"

Skew : Approx. 90°

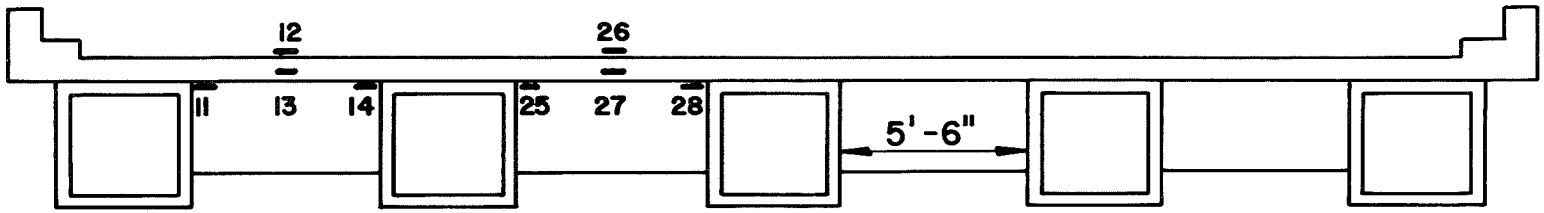

Section of Maximum Moment (M)

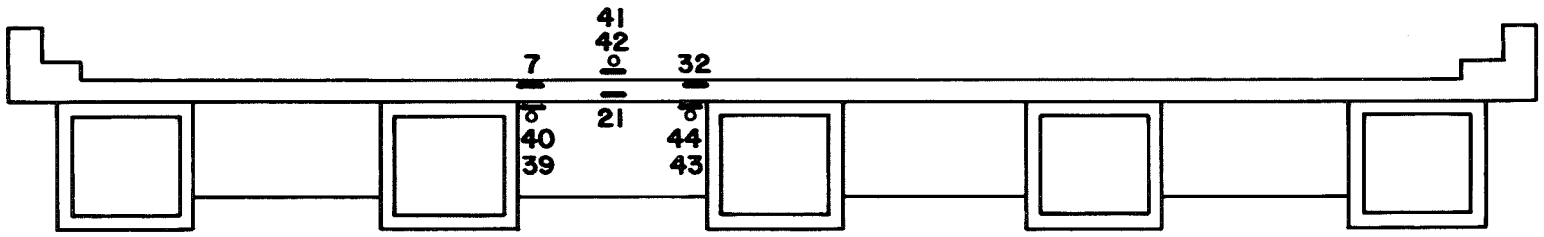

Quarter Span Section (Q)

— Transverse Gage

o Longitudinal Gage

Fig. 4b Location of Slab Gages

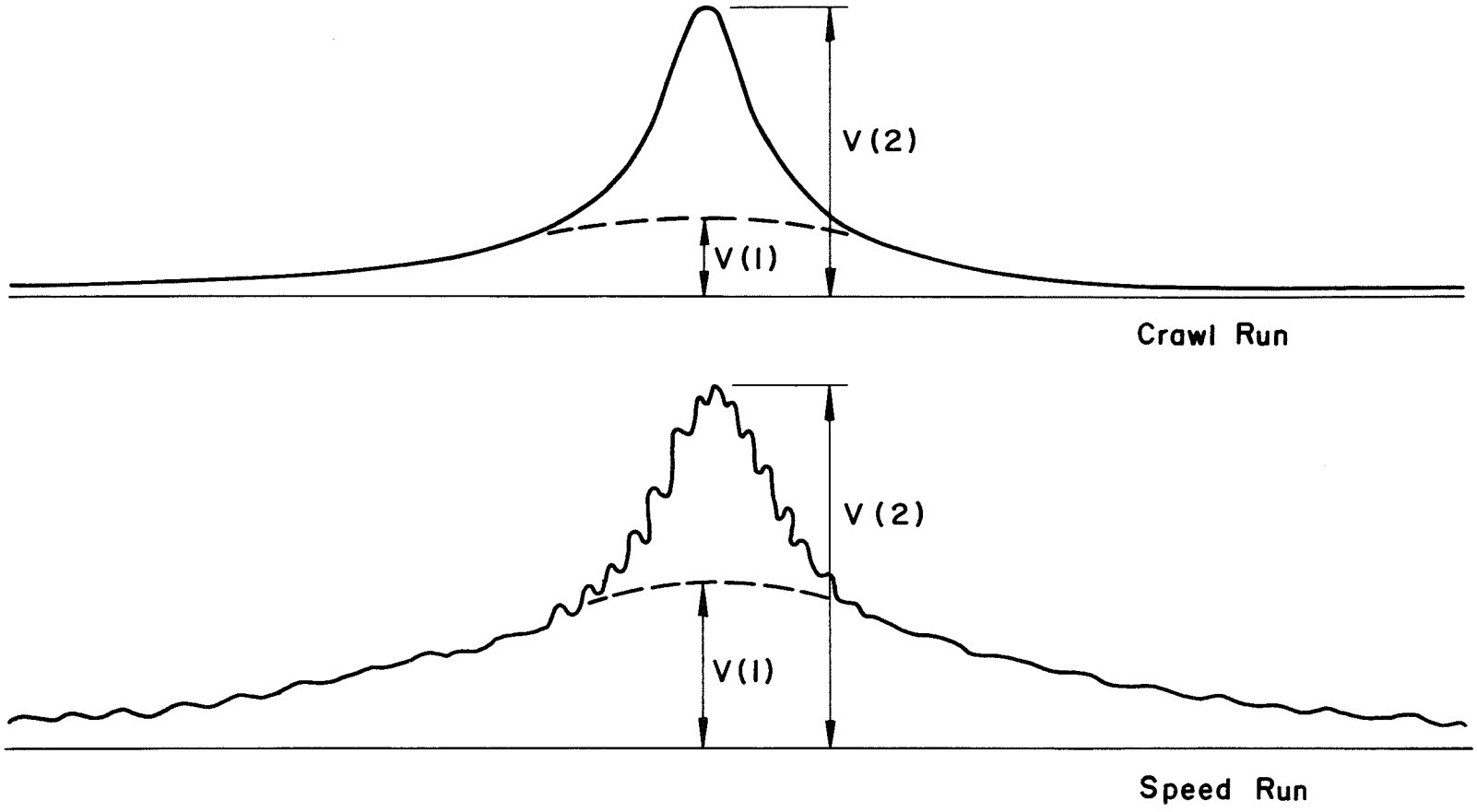

Fig. 5 Typical Oscillograph Traces

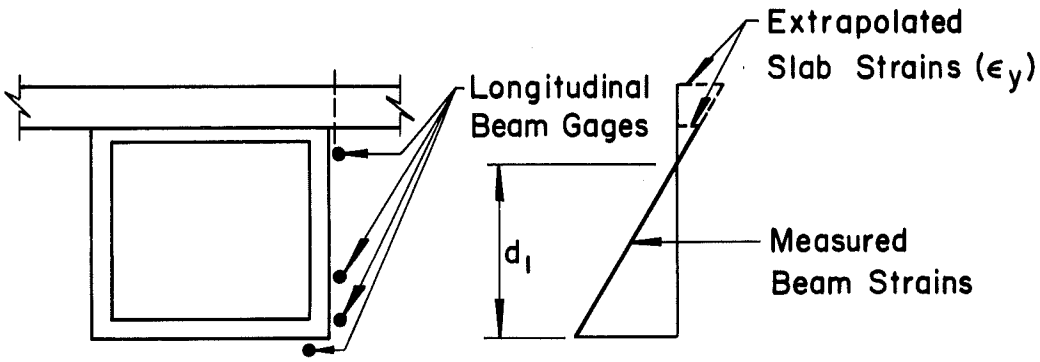

SECTION OF MAXIMUM MOMENT (M)

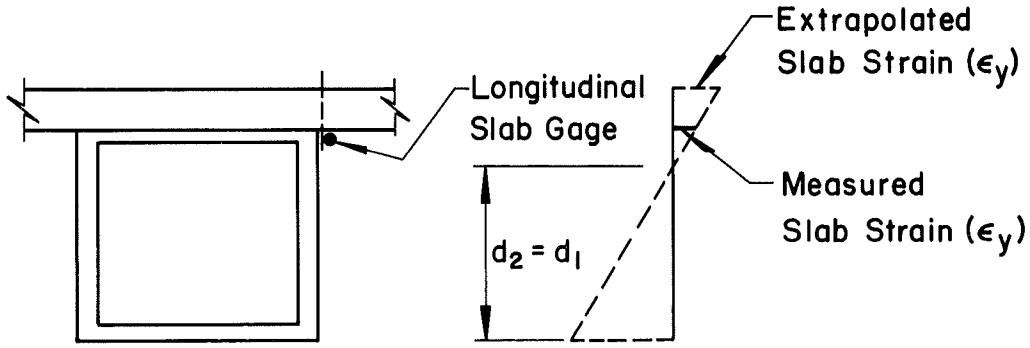

QUARTER SPAN SECTION (Q)

Fig. 6 Extrapolation of Longitudinal Slab Strains (ϵ_y) Using Beam Strains

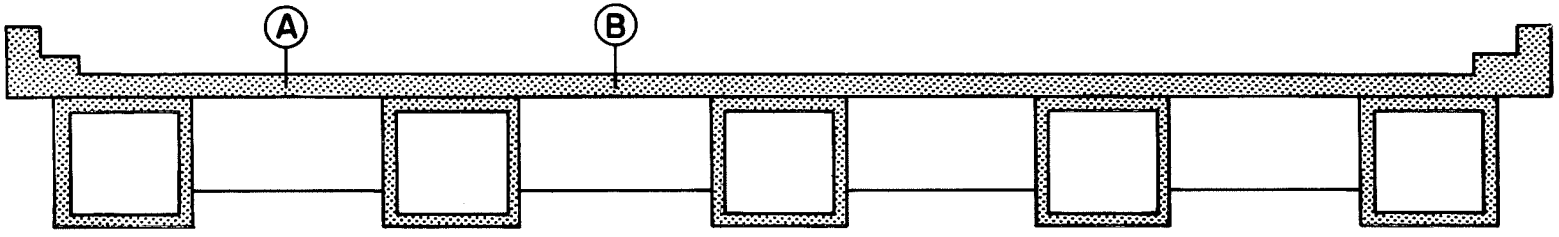

SECTION OF MAXIMUM MOMENT (M)

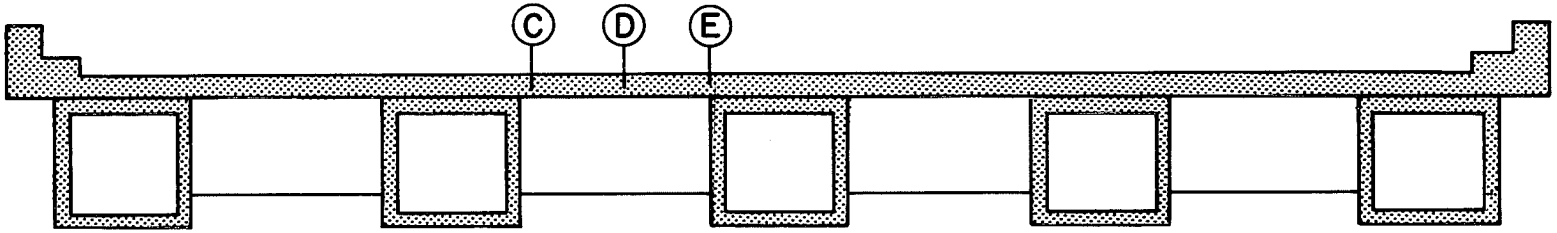

QUARTER SPAN SECTION (Q)

(For correlation of strain gage reference numbers with Sections A, B, C, D, and E, see Fig. 4b)

Fig. 7 Location of Sections Selected for Moment Computation

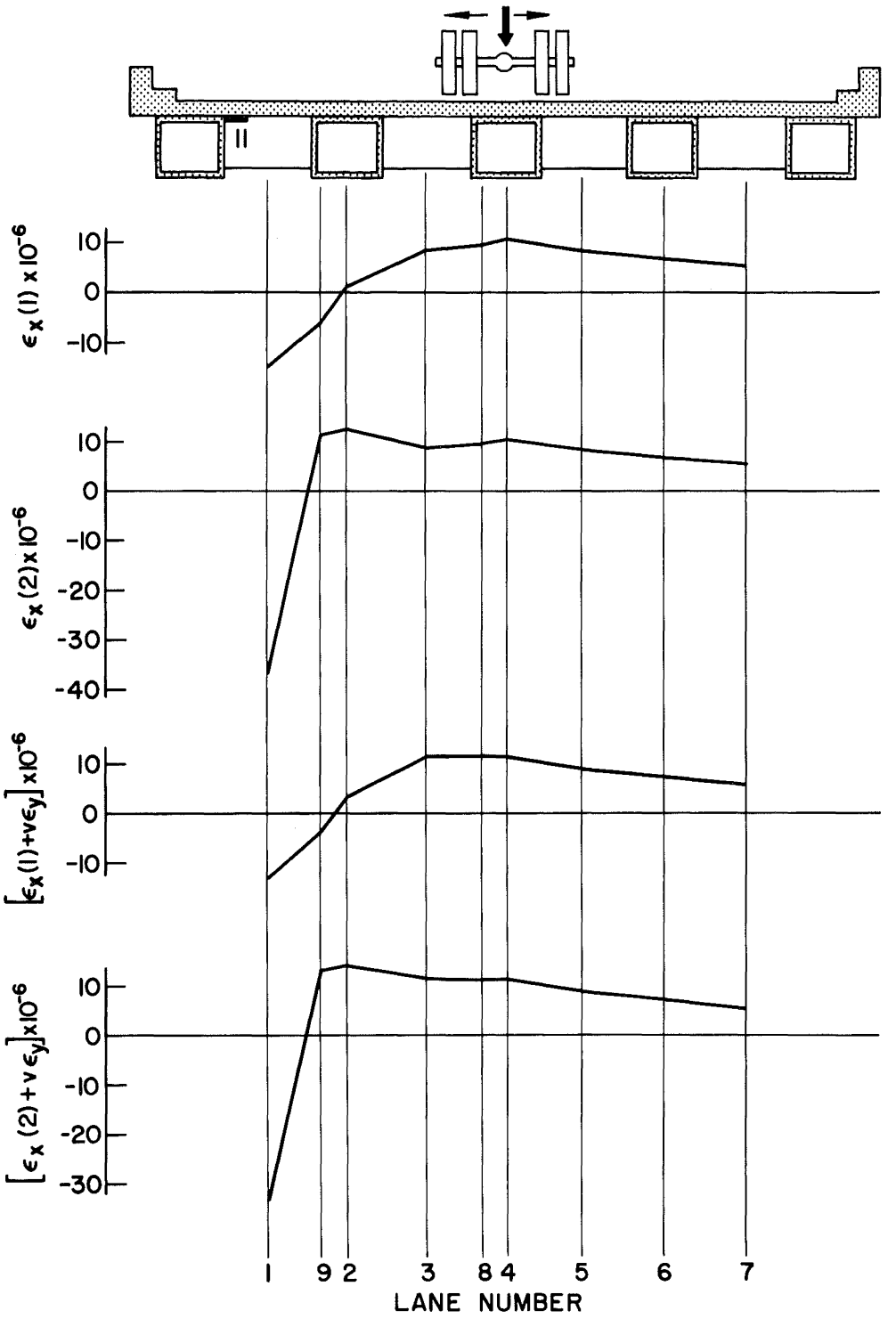

Fig. 8 Influence Lines for Transverse Strains and Stresses - Gage 11

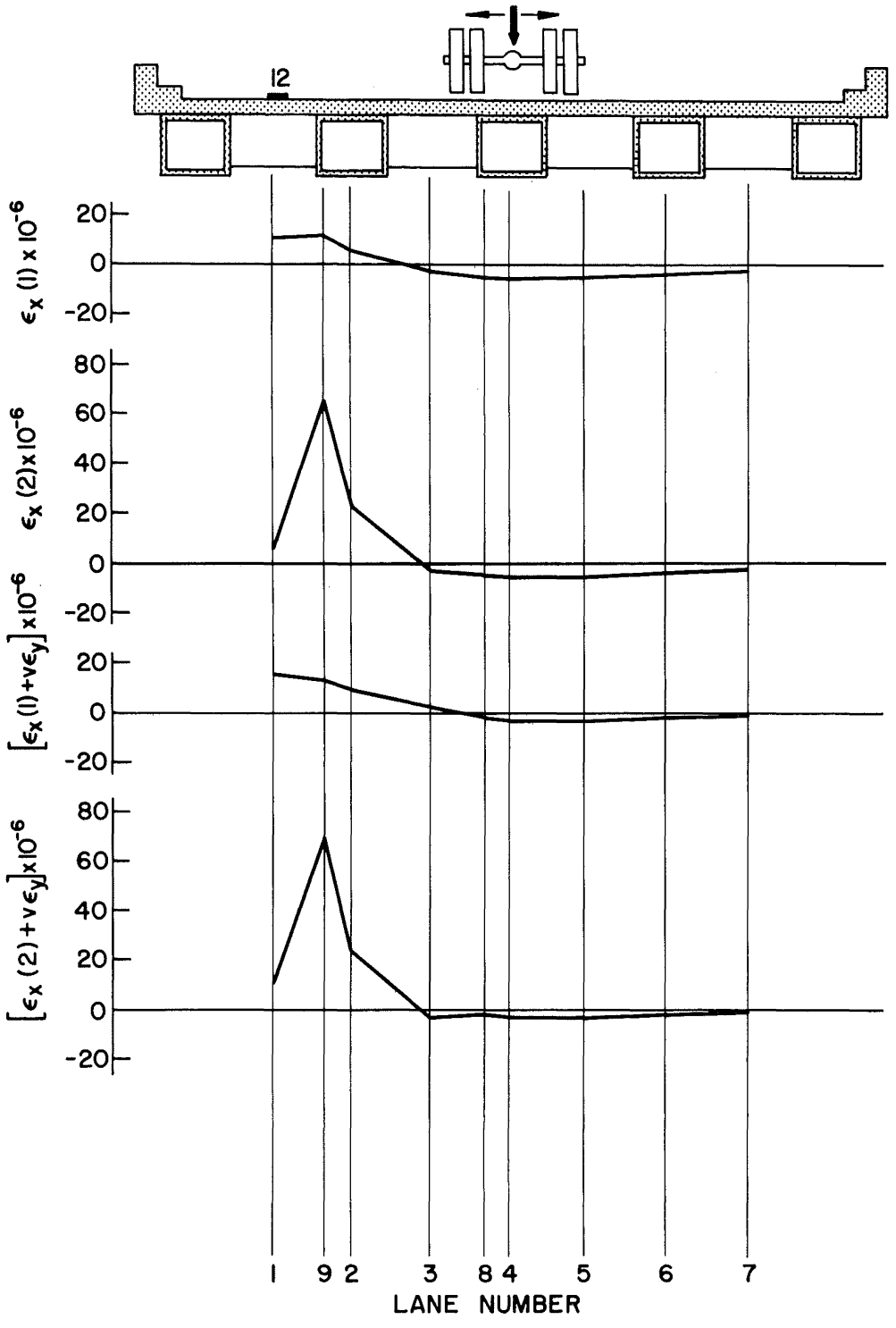

Fig. 9 Influence Lines for Transverse Strains and Stresses - Gage 12

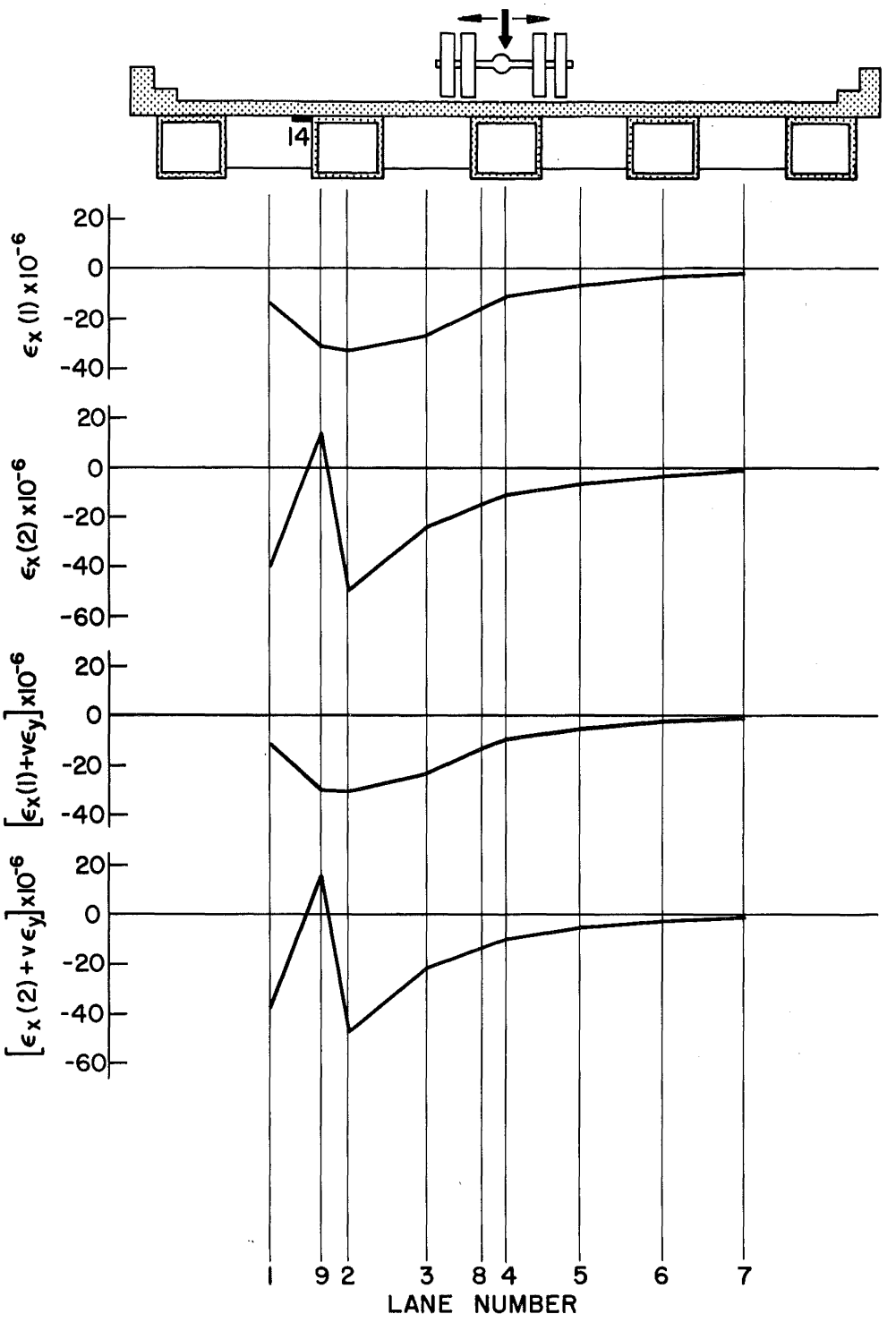

Fig. 10 Influence Lines for Transverse Strains and Stresses - Gage 14

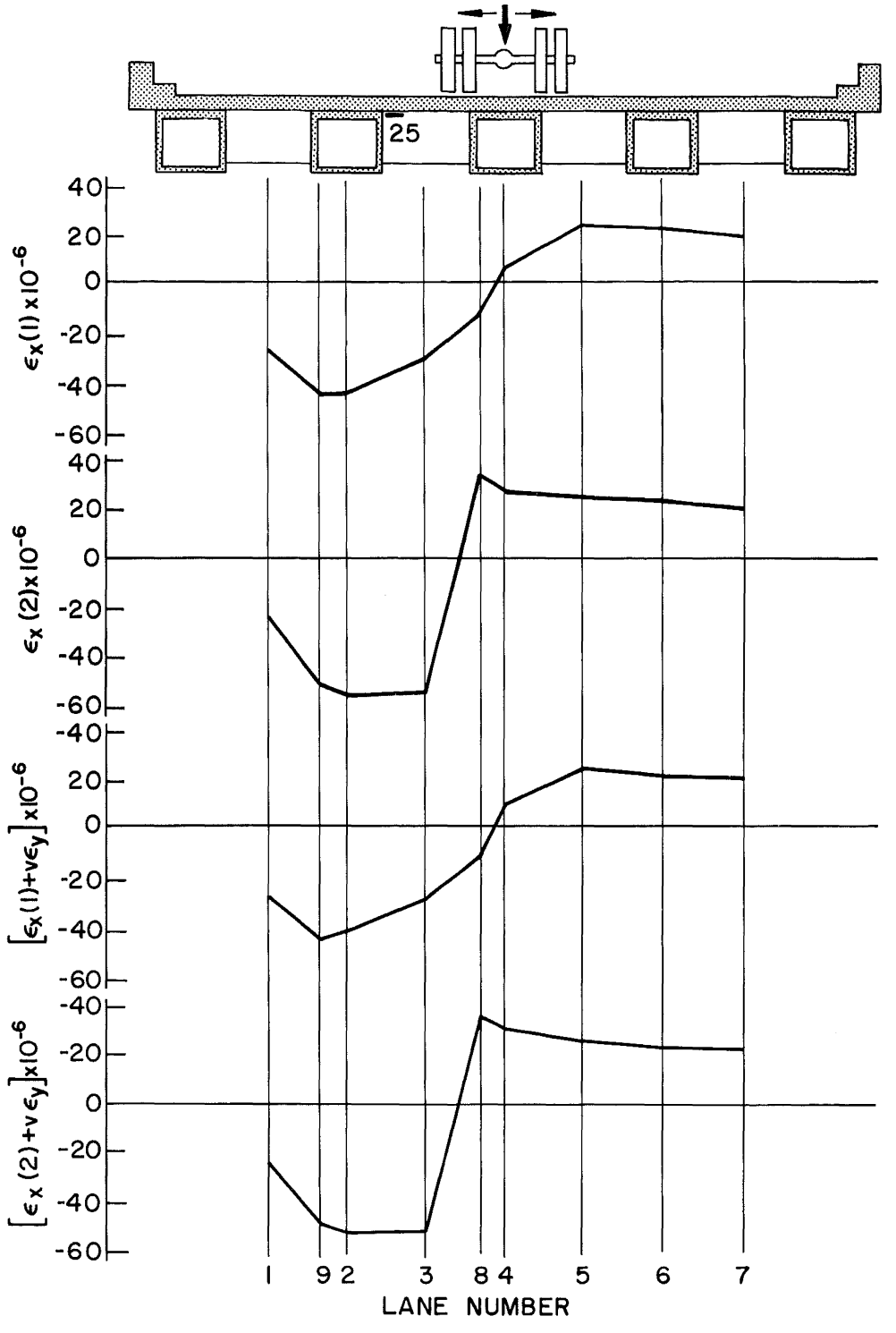

Fig. 11 Influence Lines for Transverse Strains and Stresses - Gage 25

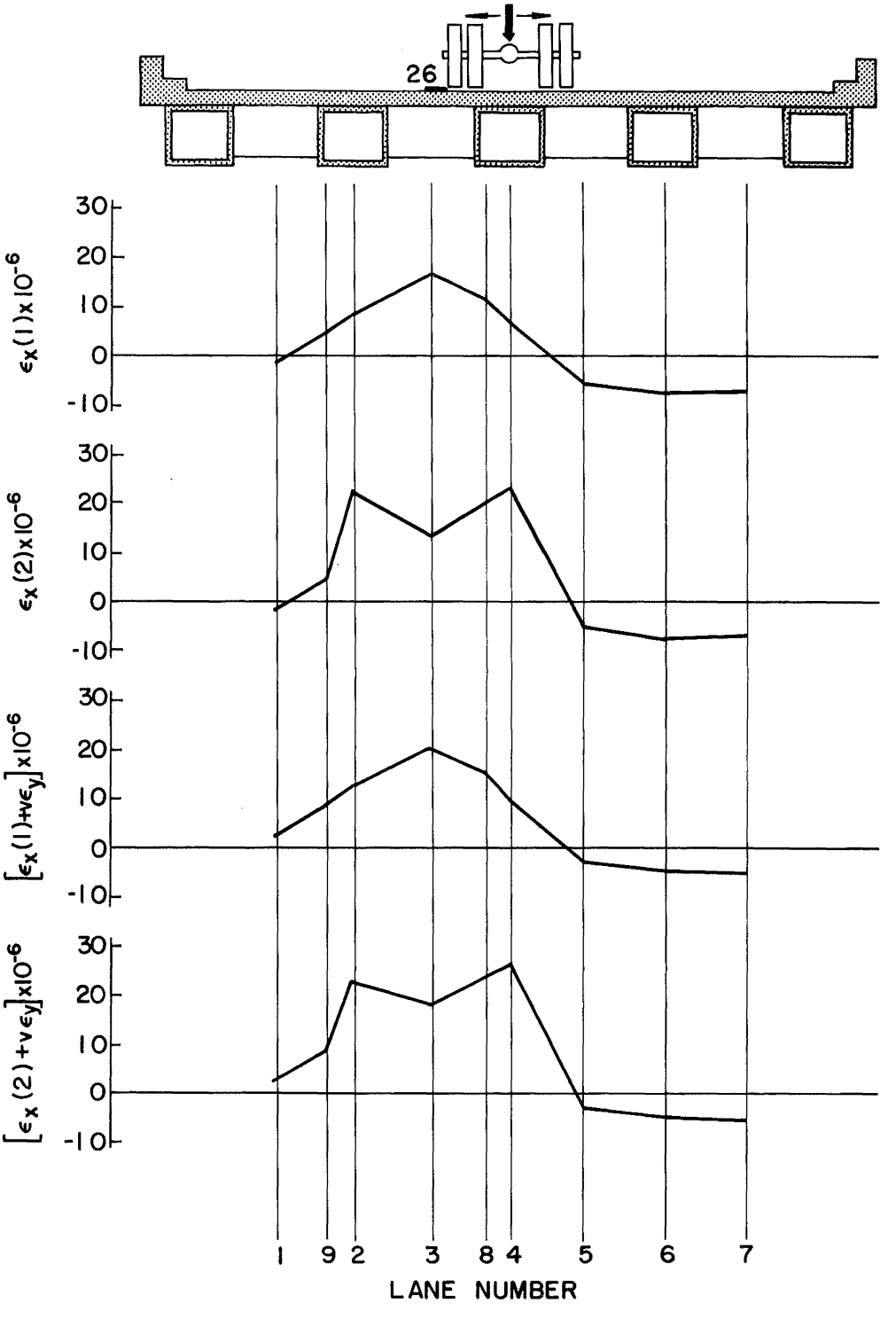

Fig. 12 Influence Lines for Transverse Strains and Stresses - Gage 26

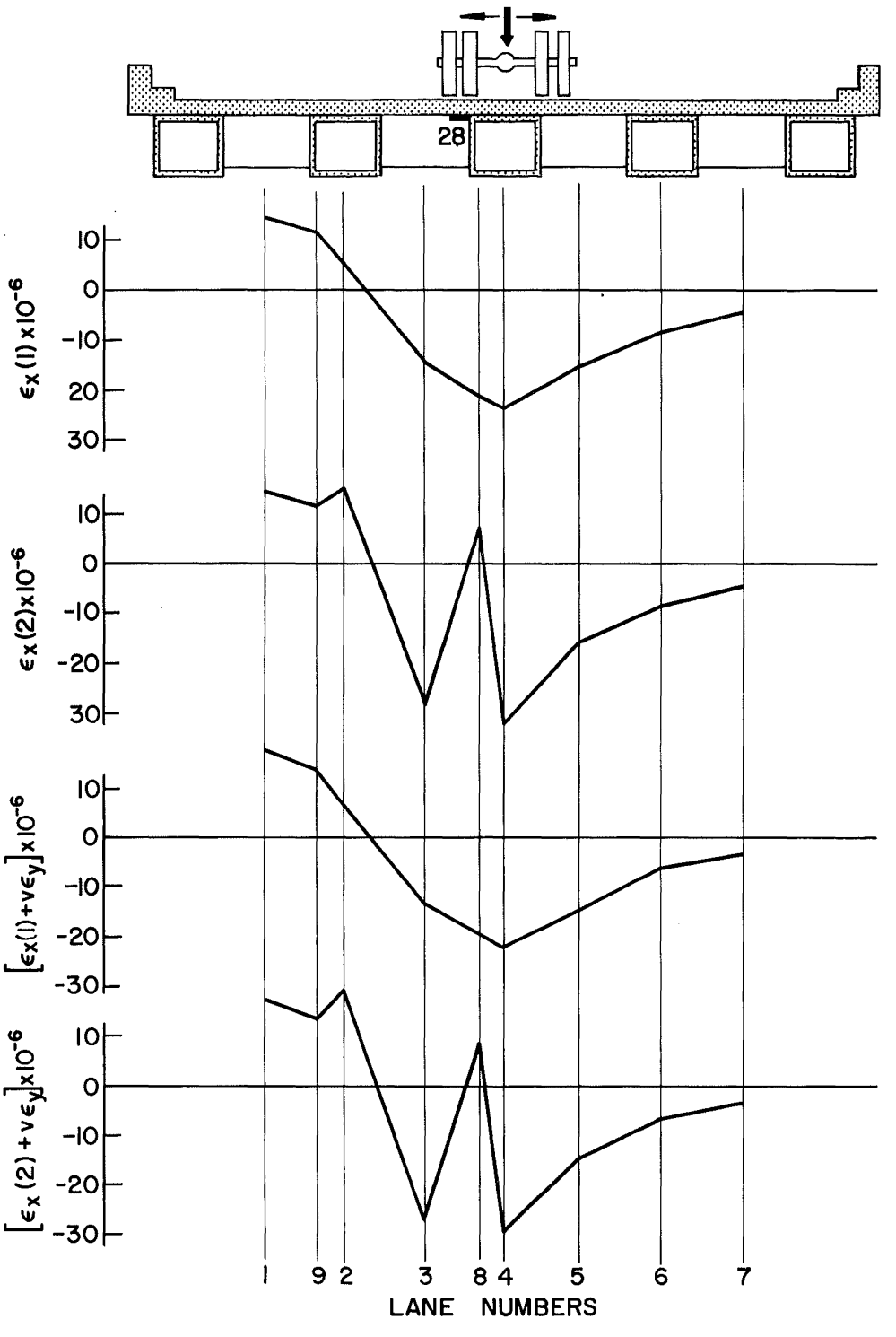

Fig. 13 Influence Lines for Transverse Strains and Stresses - Gage 28

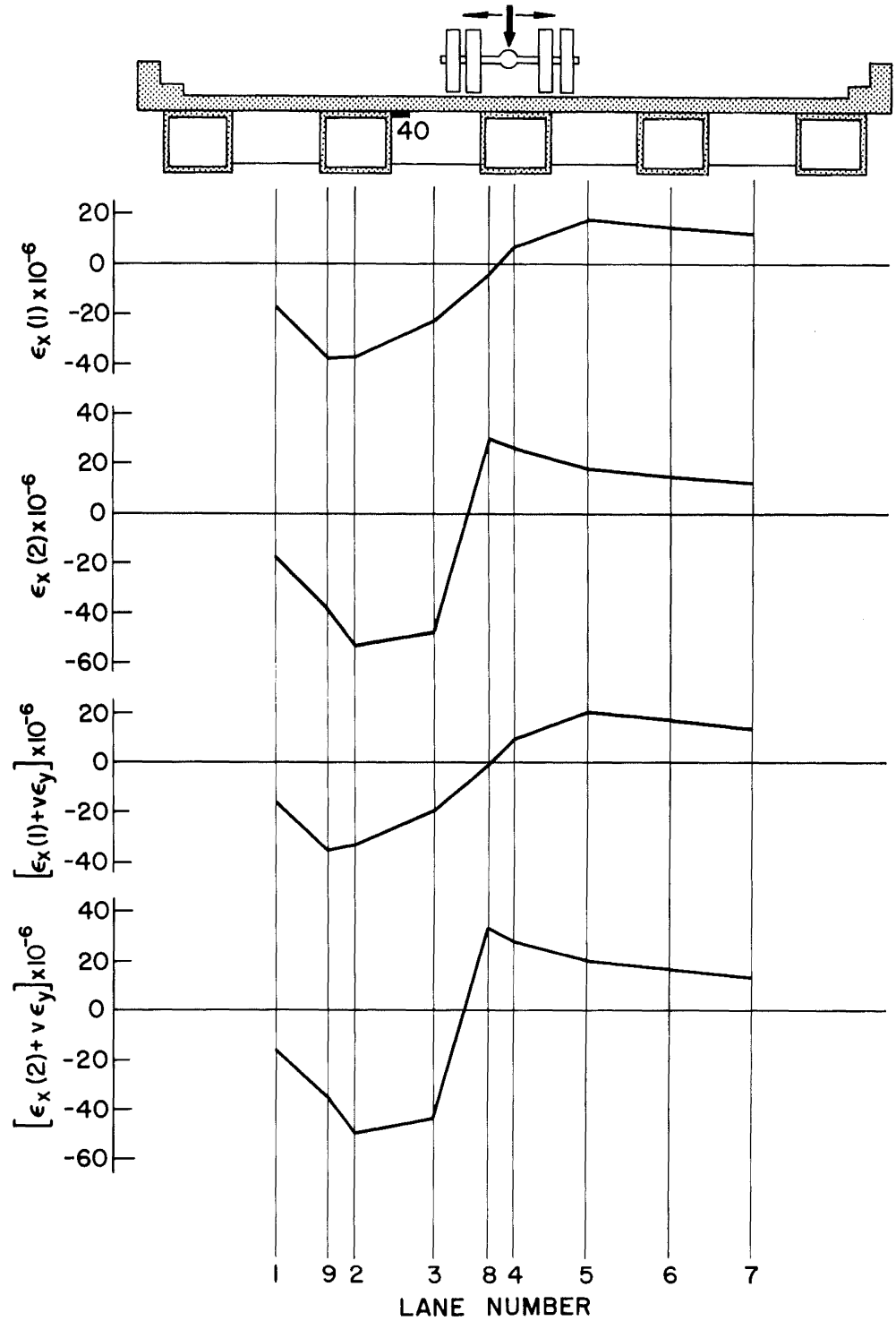

Fig. 14 Influence Lines for Transverse Strains and Stresses - Gage 40

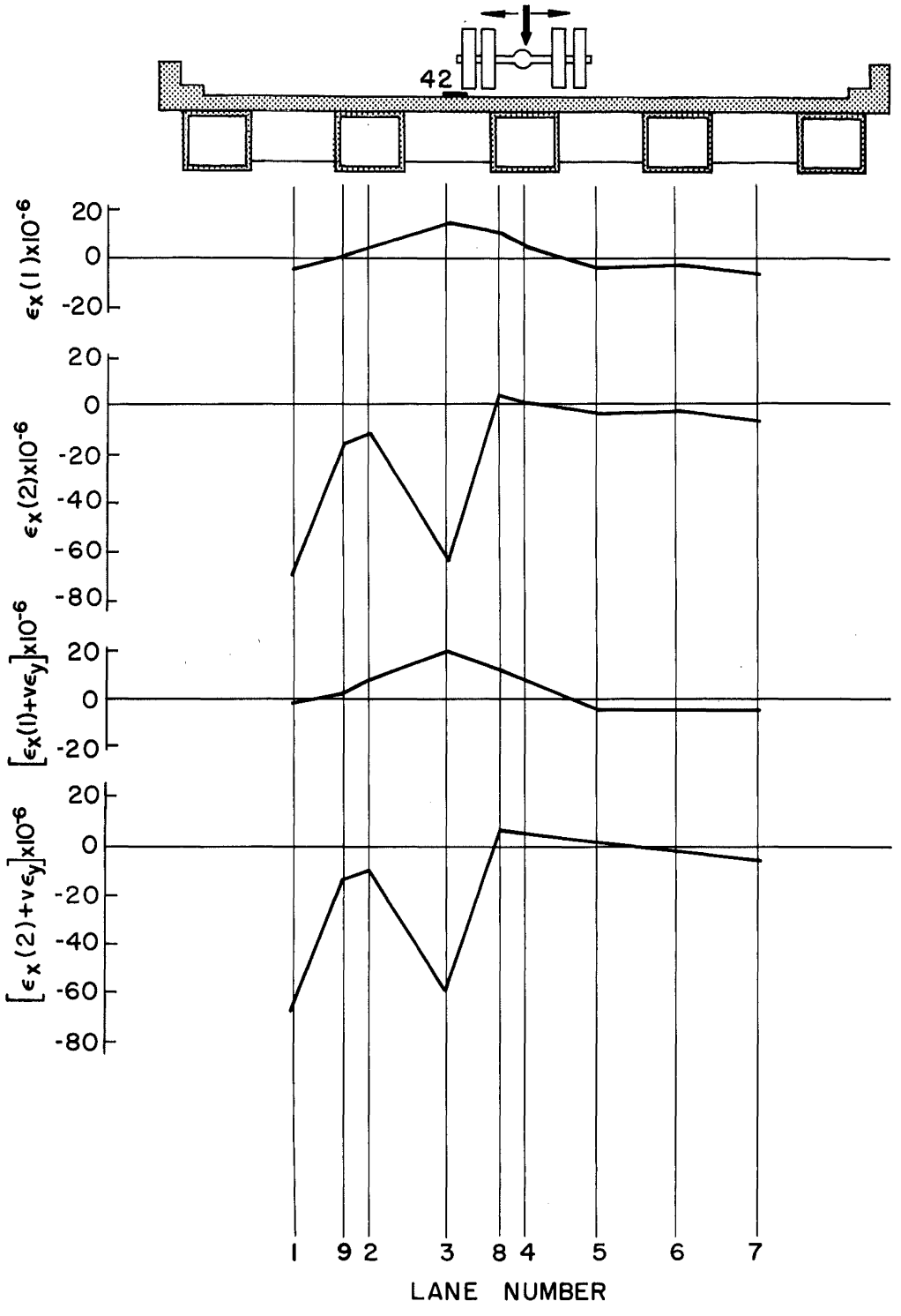

Fig. 15 Influence Lines for Transverse Strains and Stresses - Gage 42

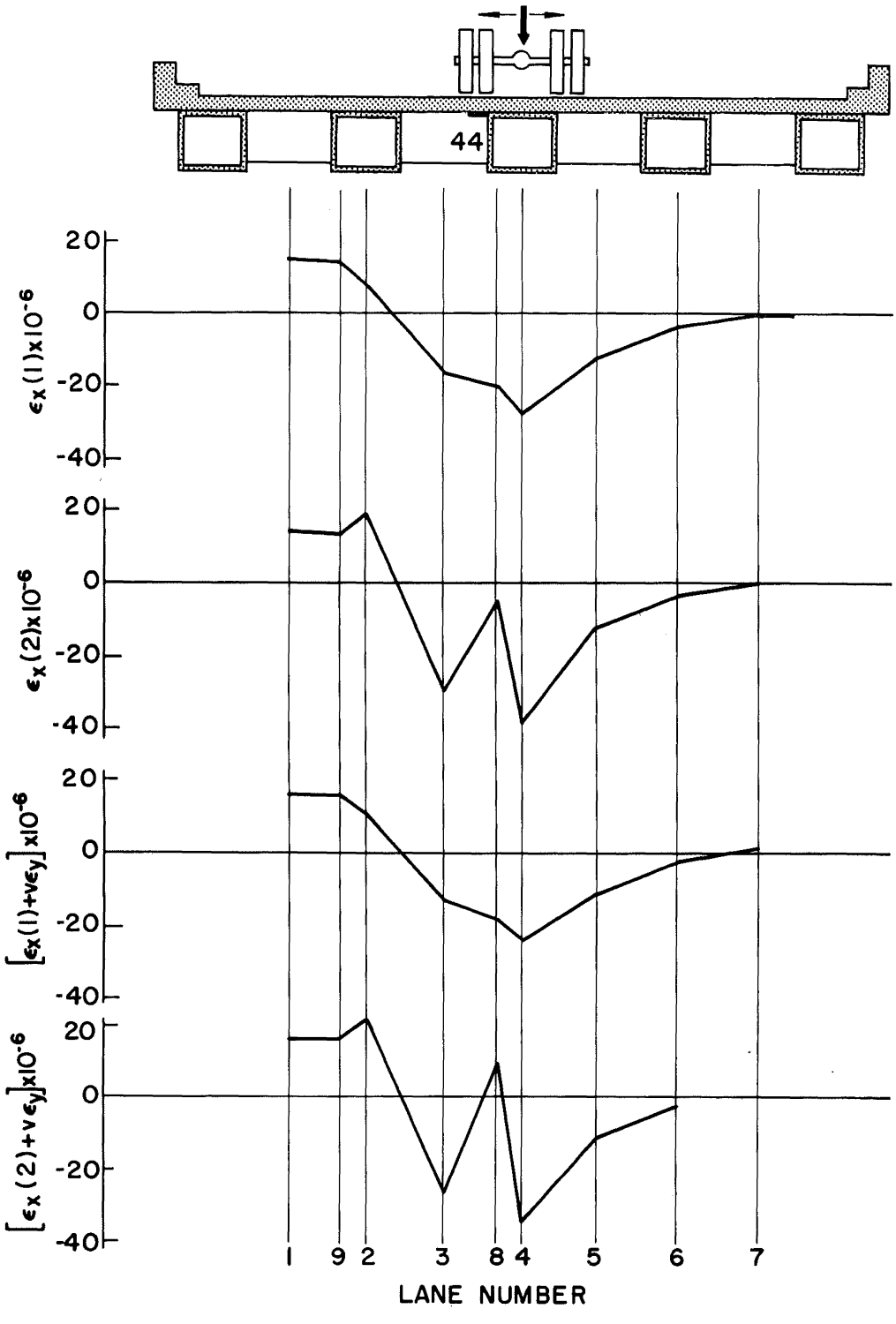

Fig. 16 Influence Lines for Transverse Strains and Stresses - Gage 44

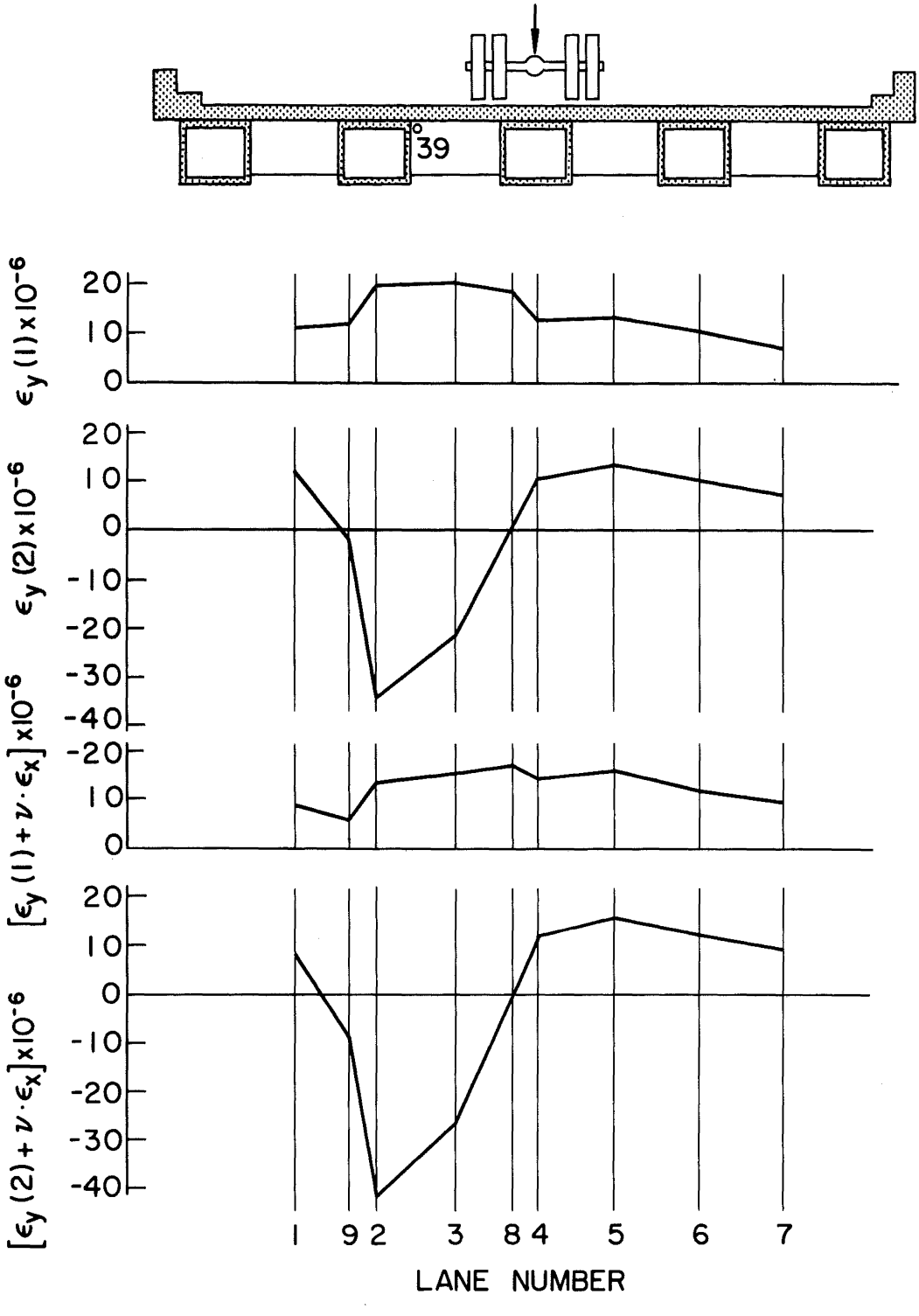

Fig. 17 Influence Lines for Longitudinal Strains and Stresses - Gage 39

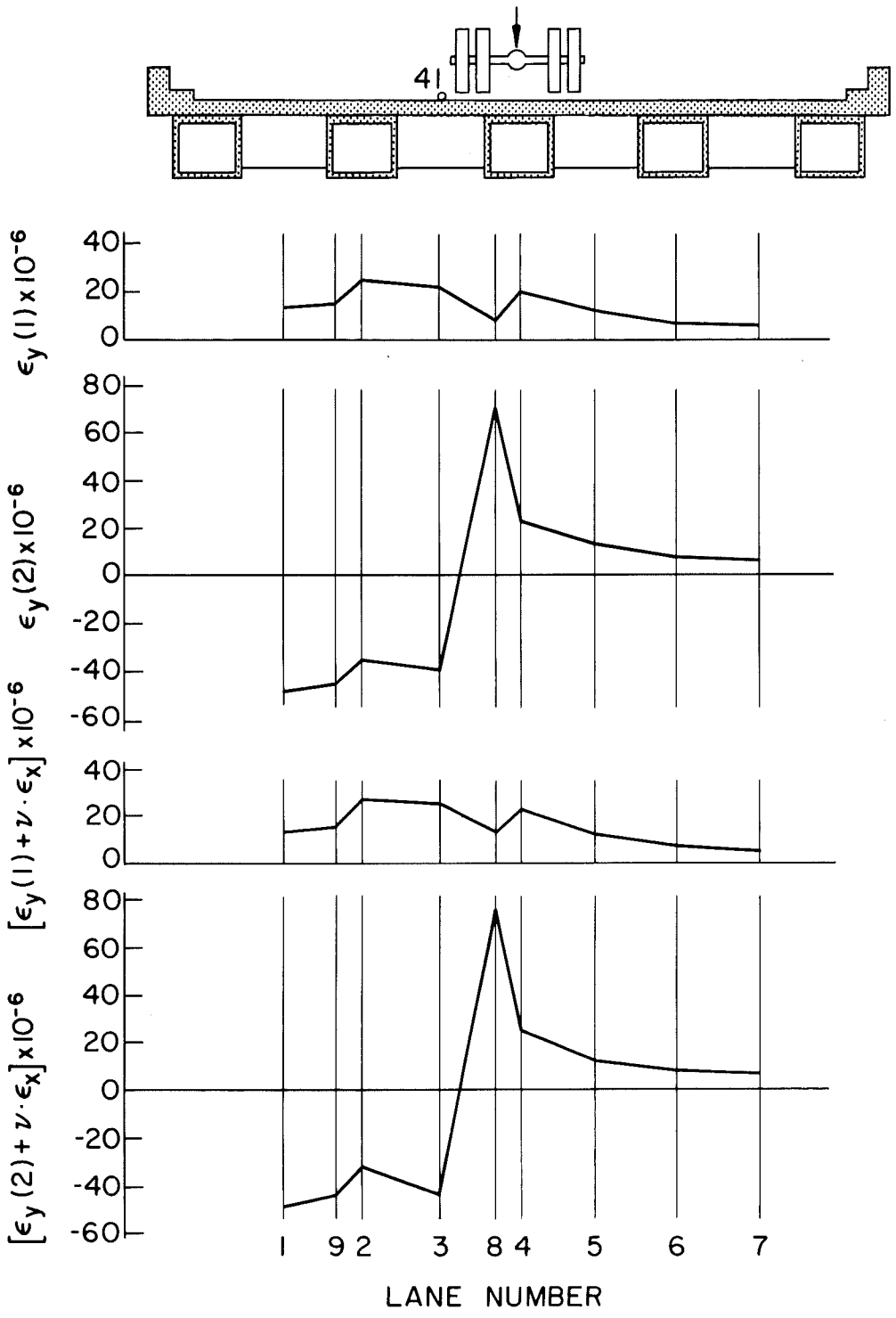

Fig. 18 Influence Lines for Longitudinal Strains and Stresses - Gage 41

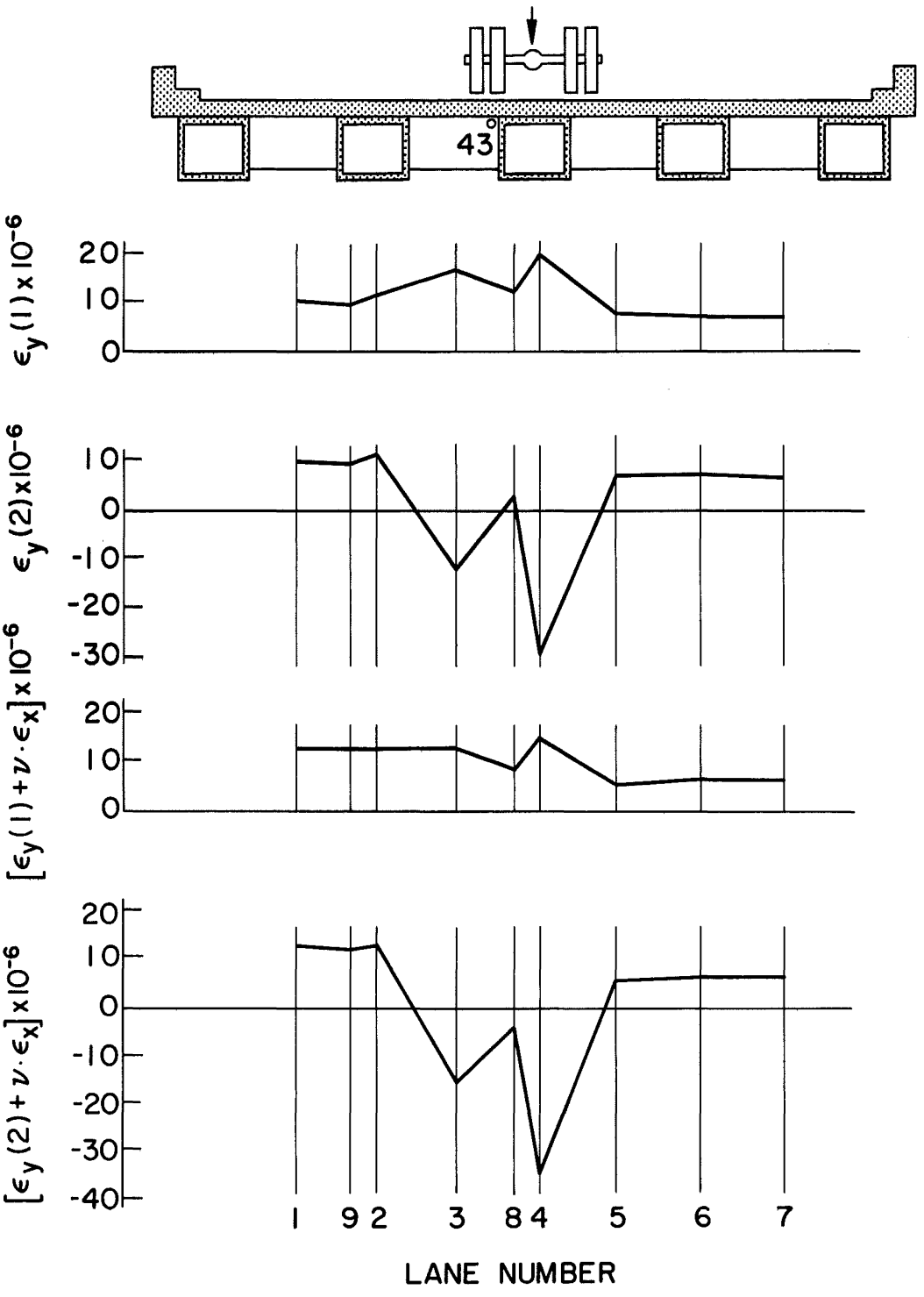

Fig. 19 Influence Lines for Longitudinal Strains and Stresses - Gage 43

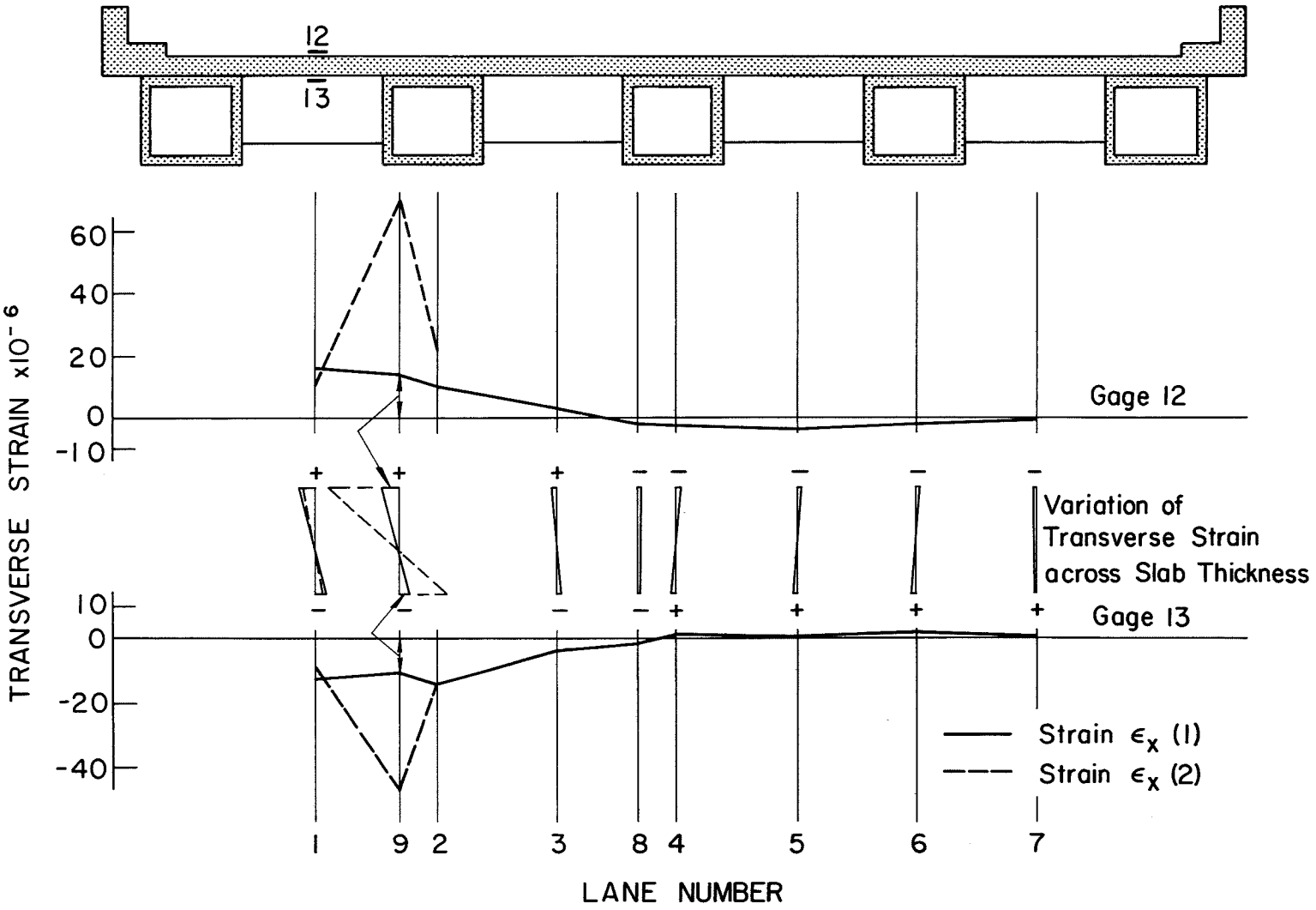

Fig. 20 Variation of Transverse Strain Across Slab Thickness - Gages 12 and 13

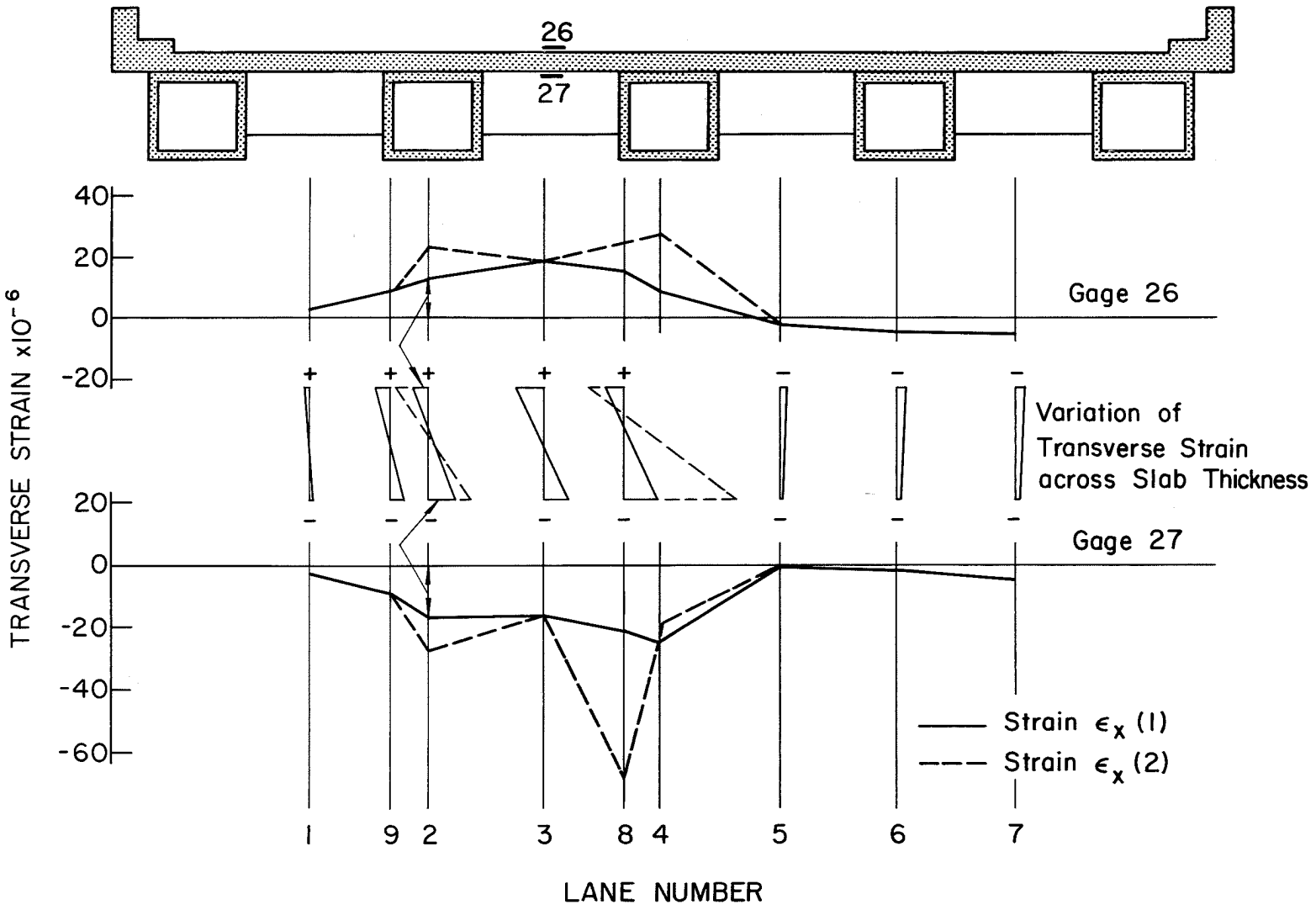

Fig. 21 Variation of Transverse Strain Across Slab Thickness - Gages 26 and 27

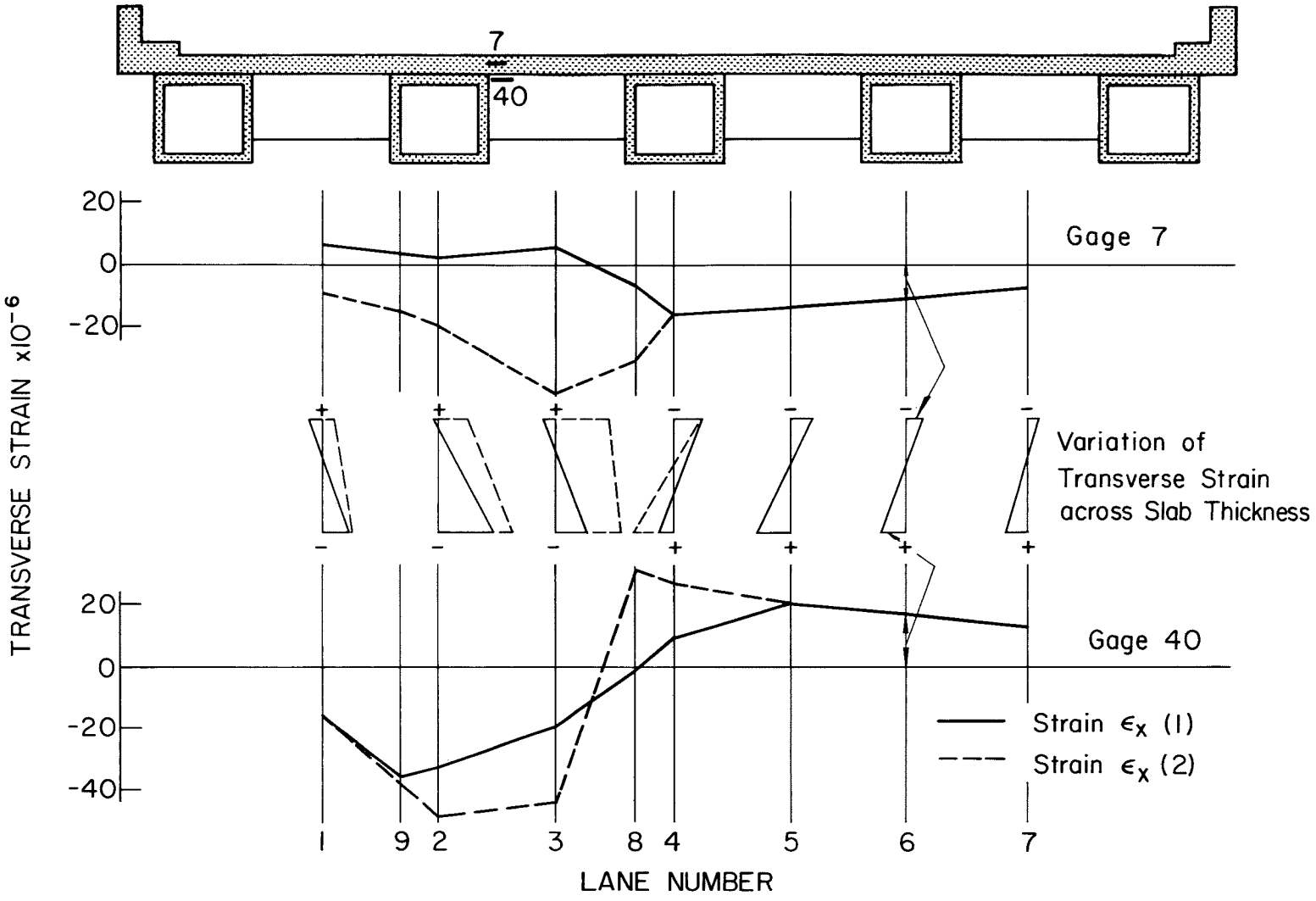

Fig. 22 Variation of Transverse Strain Across Slab Thickness - Gages 7 and 40

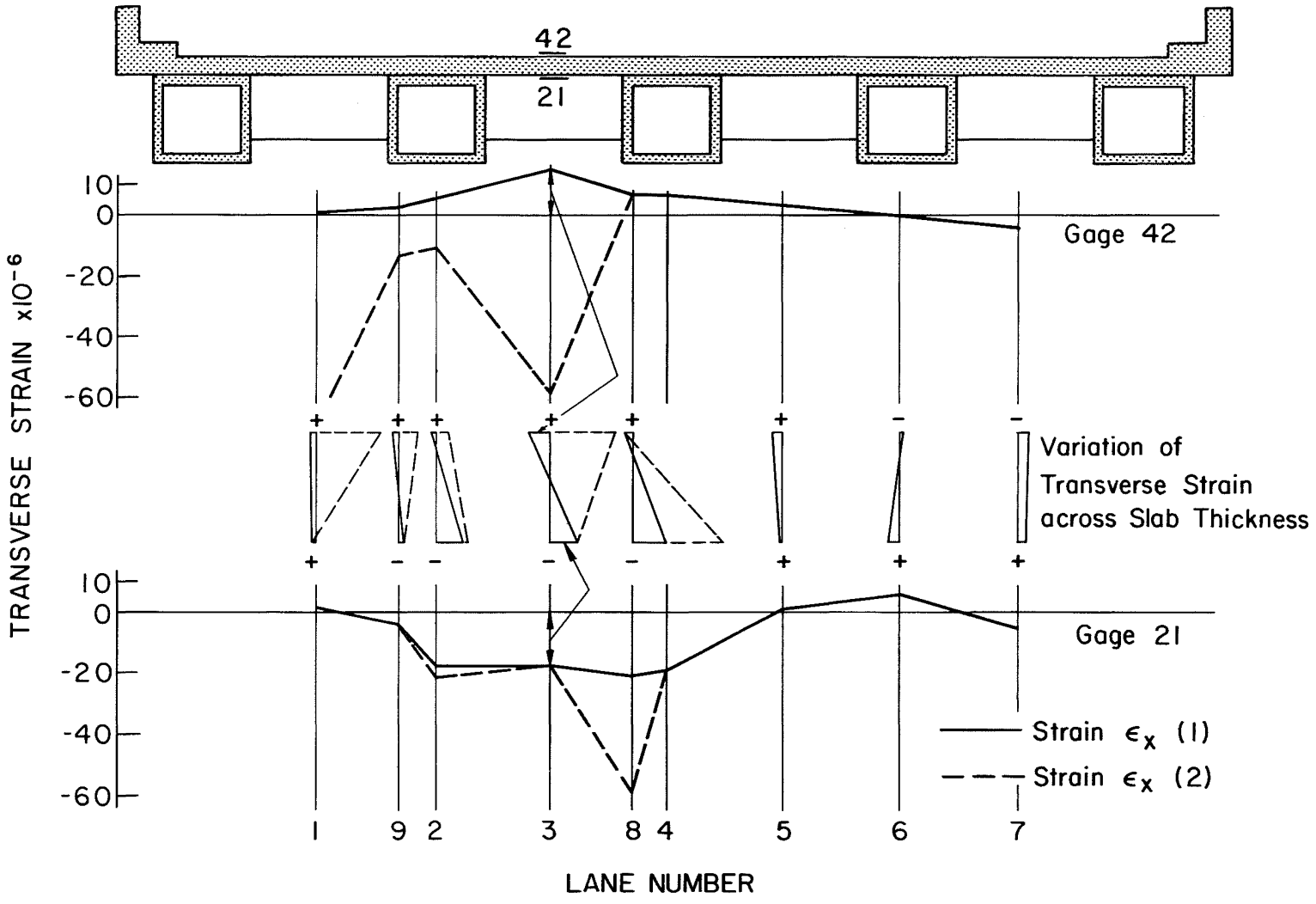

Fig. 23 Variation of Transverse Strain Across Slab Thickness - Gages 42 and 21

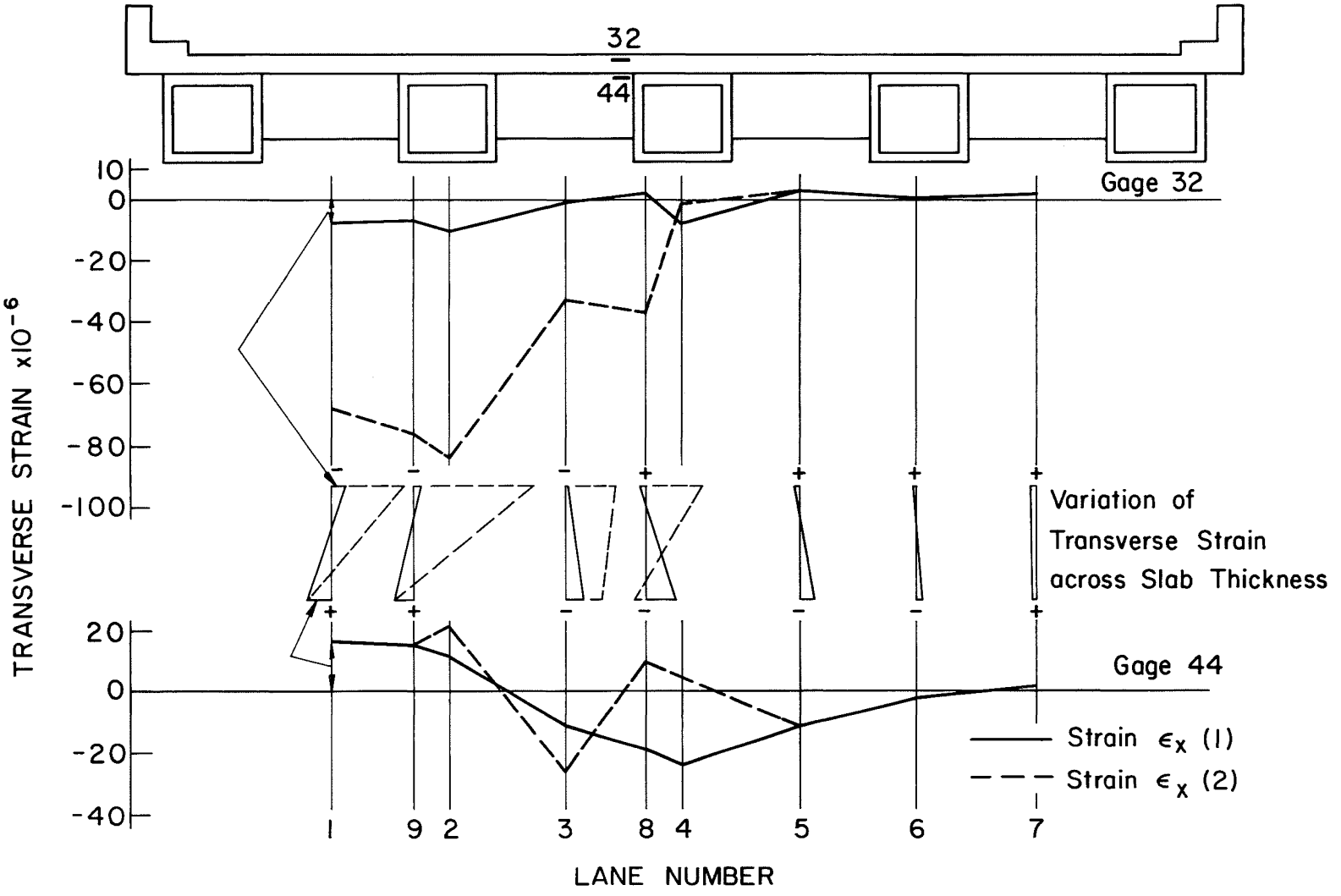

Fig. 24 Variation of Transverse Strain Across Slab Thickness - Gages 32 and 44

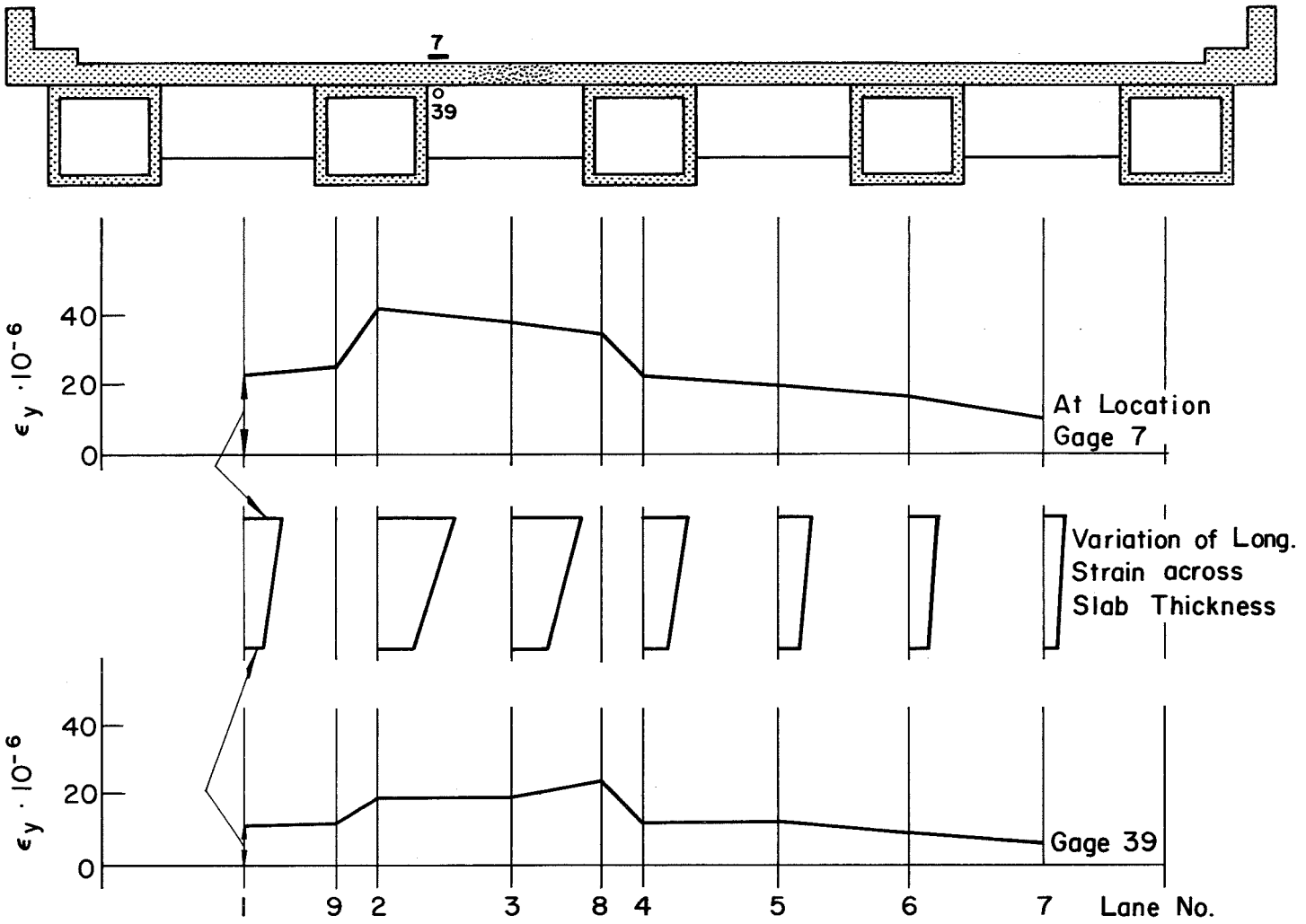

Fig. 25 Variation of Longitudinal Strain Across Slab Thickness - Gages 7 and 39

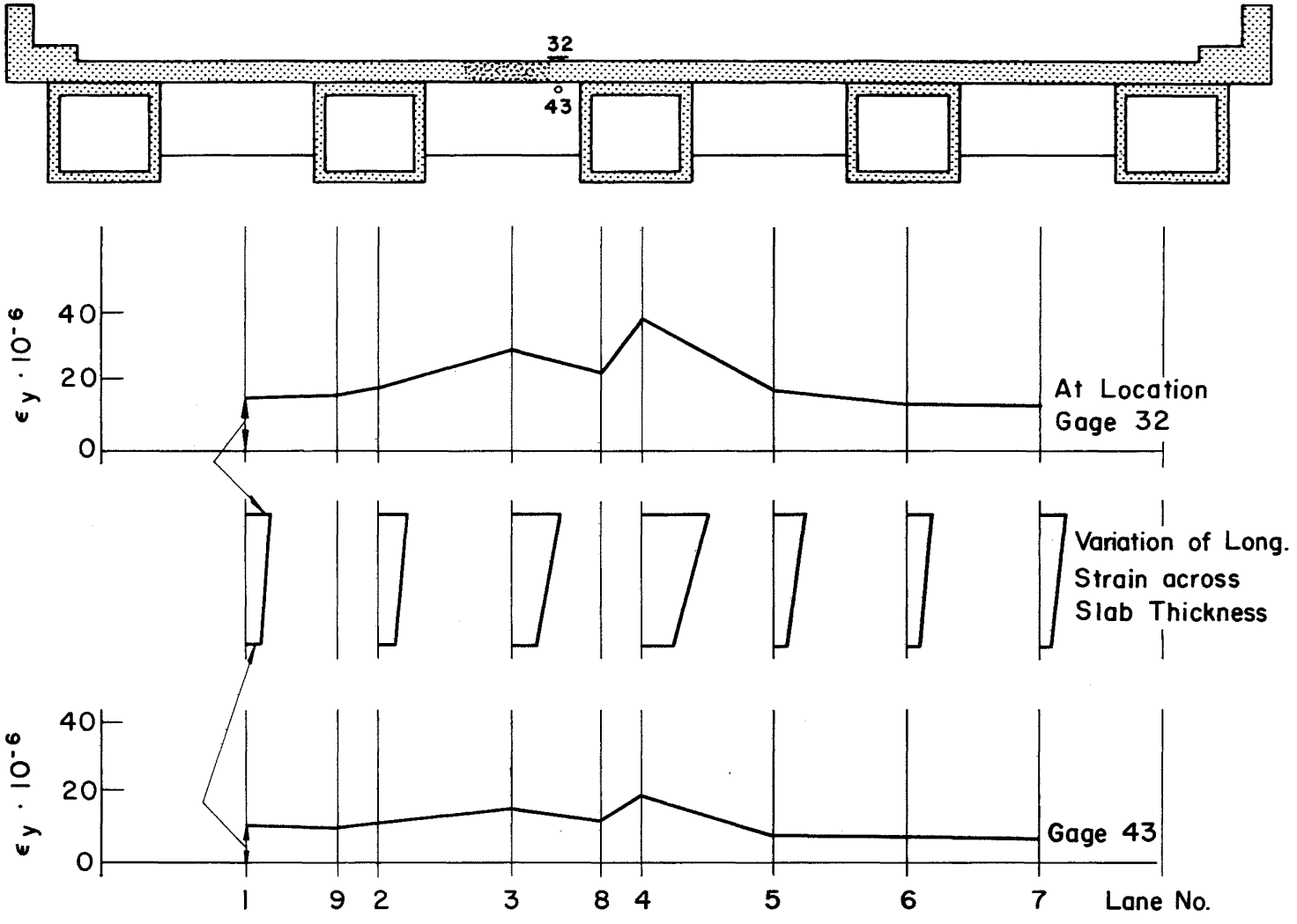

Fig. 26 Variation of Longitudinal Strain Across Slab Thickness - Gages 32 and 43

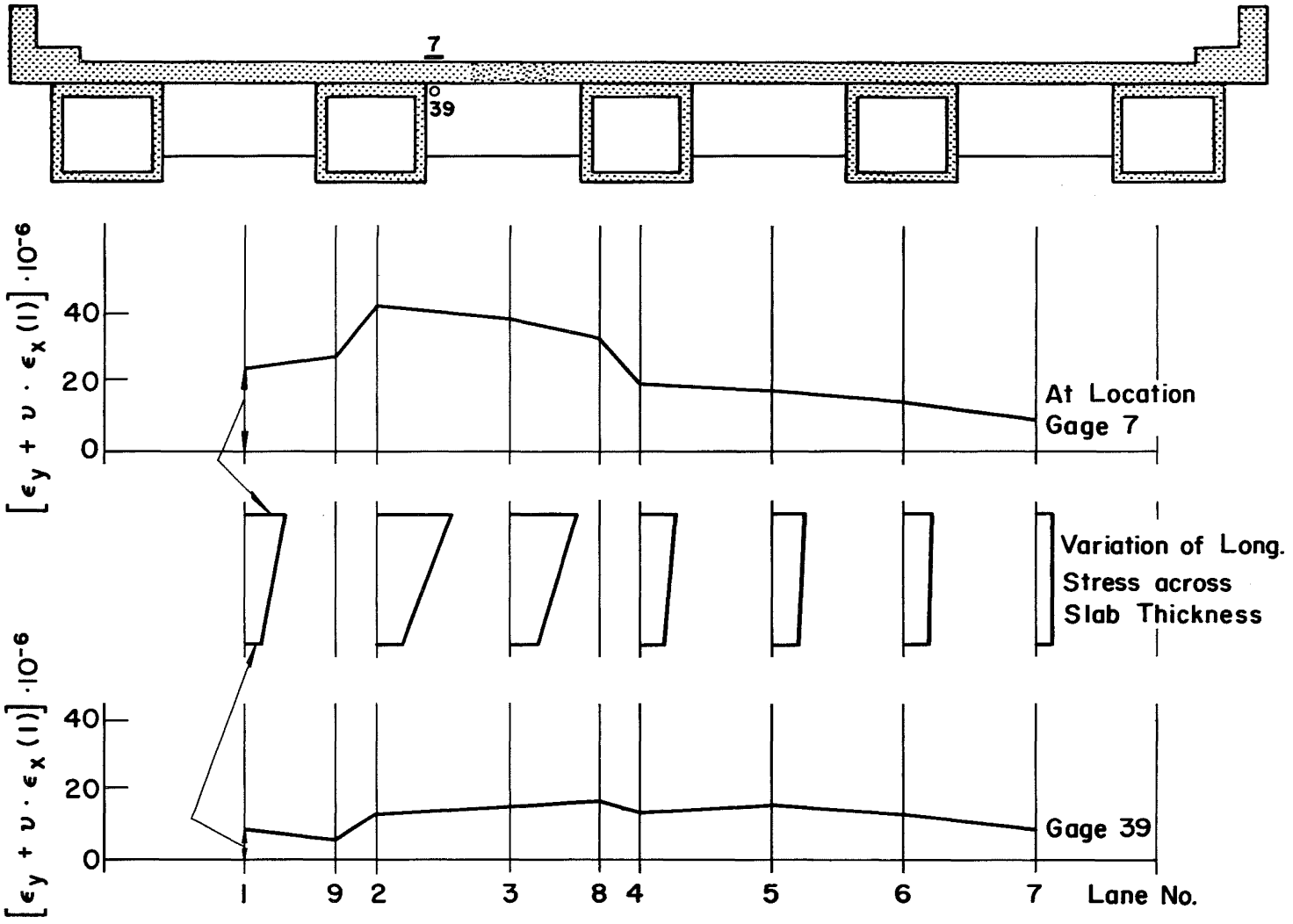

Fig. 27 Variation of Longitudinal Stress Across Slab Thickness - Gages 7 and 39

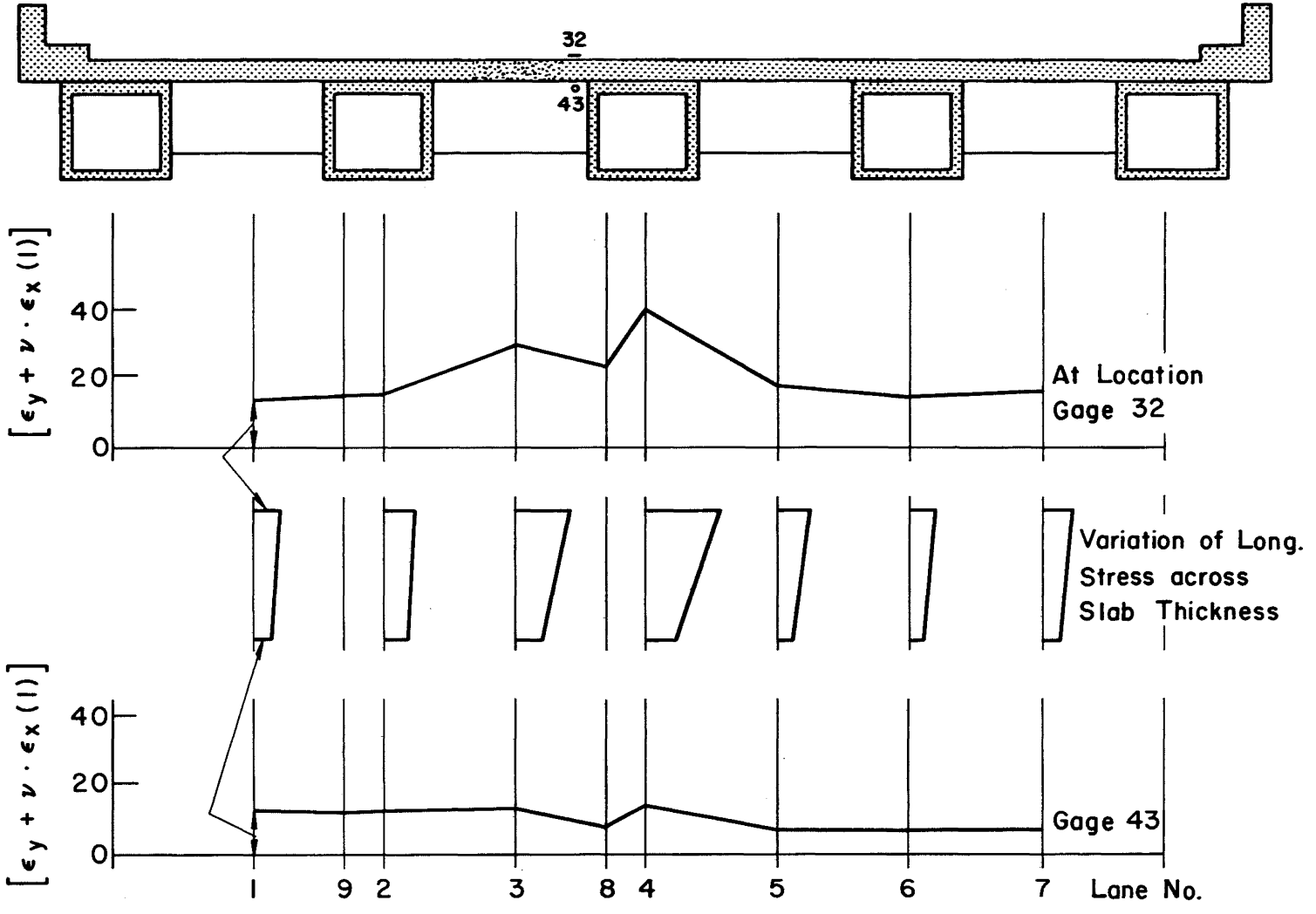

Fig. 28 Variation of Longitudinal Stress Across Slab Thickness - Gages 32 and 43

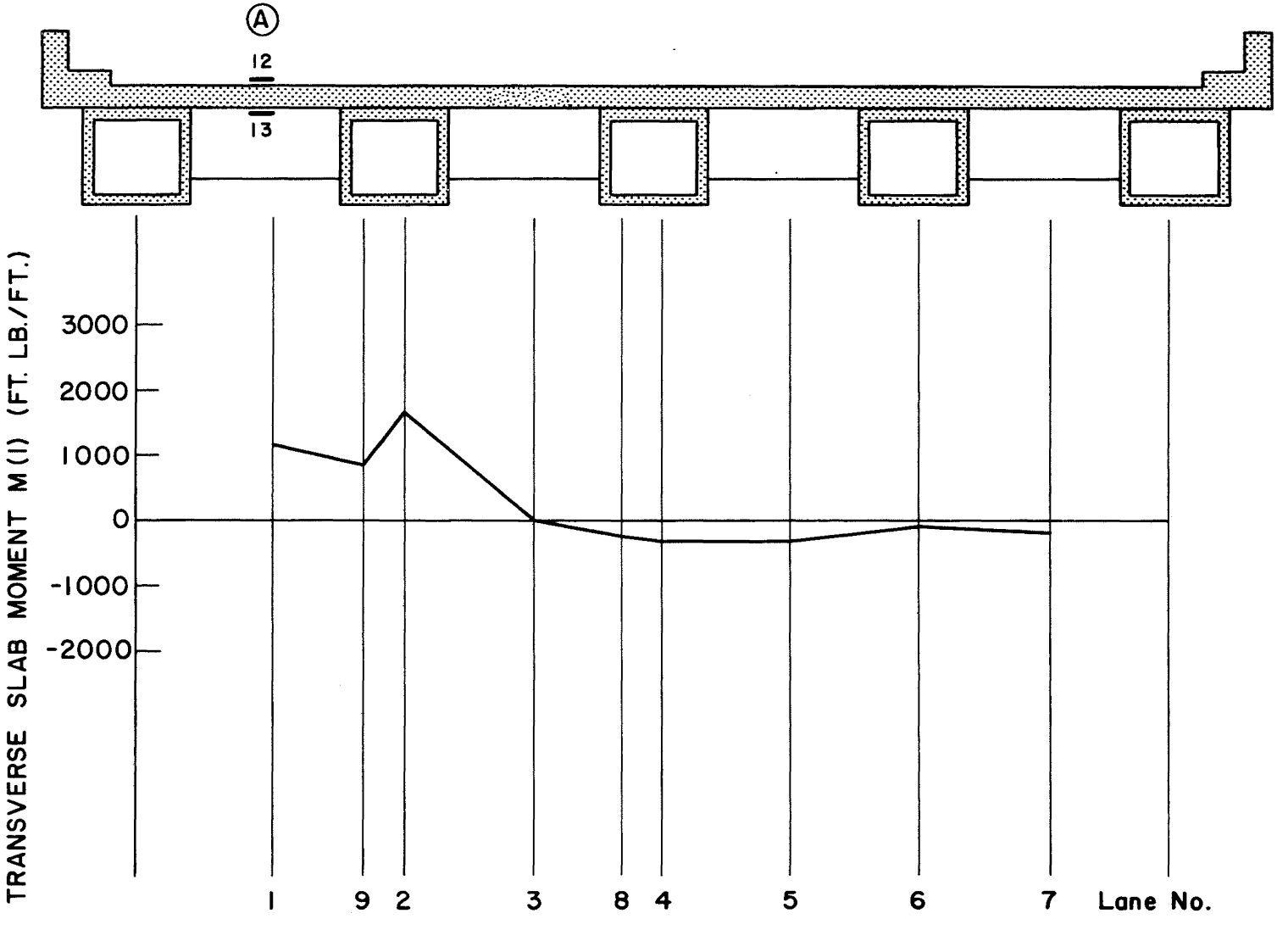

Fig. 29 Influence Lines for Transverse Slab Moments - Section A

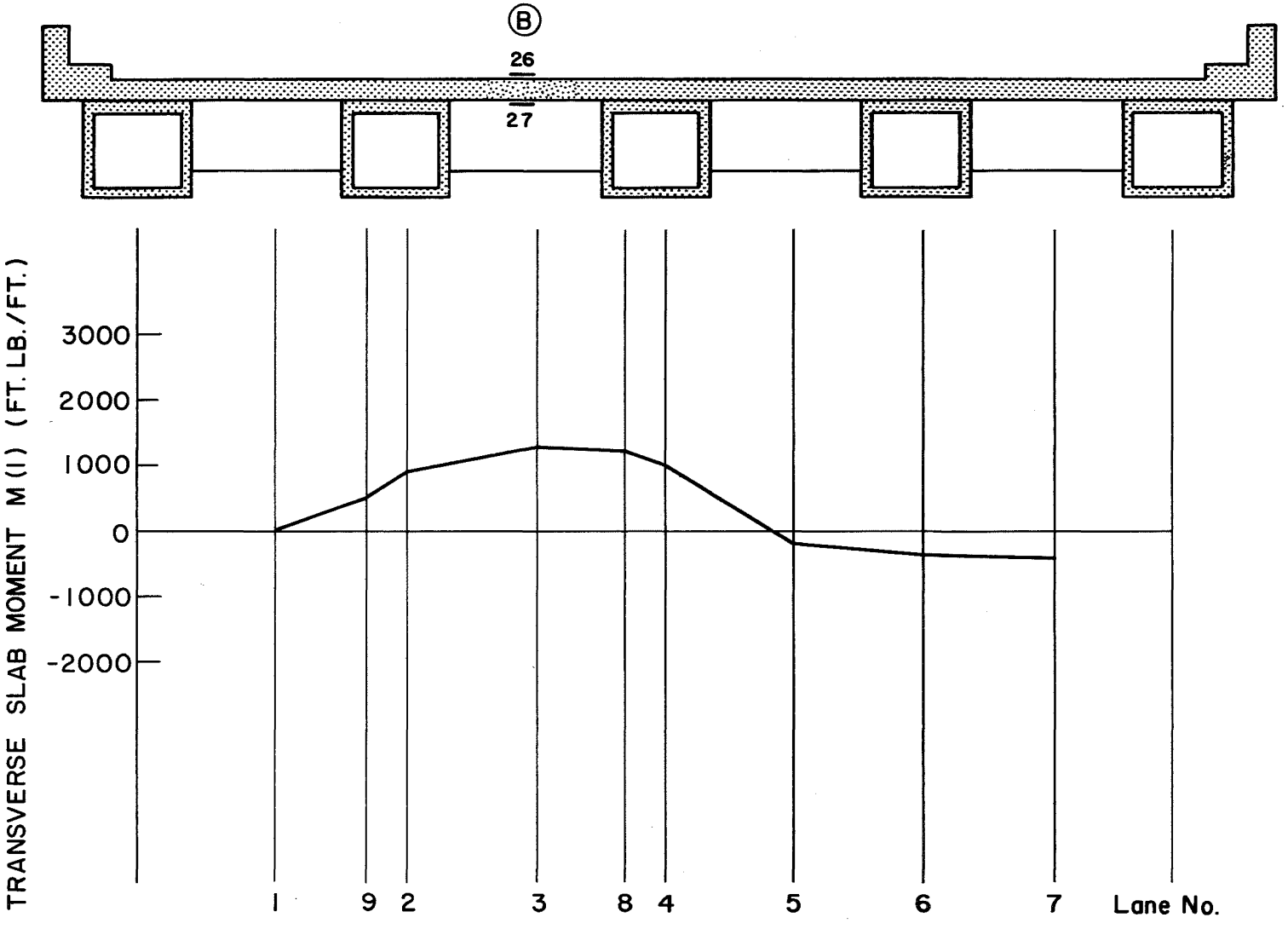

Fig. 30 Influence Lines for Transverse Slab Moments - Section B

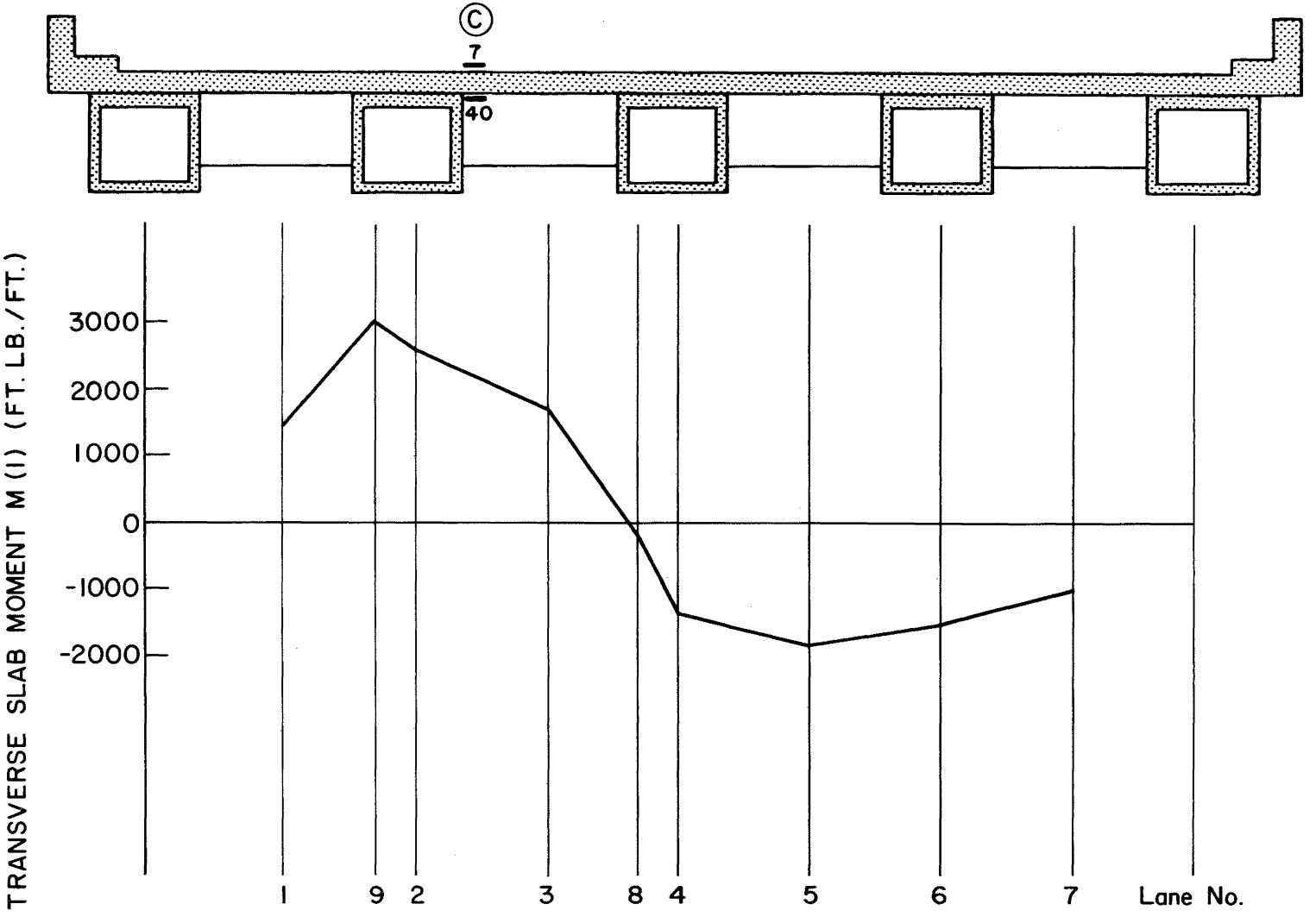

Fig. 31 Influence Lines for Transverse Slab Moments - Section C

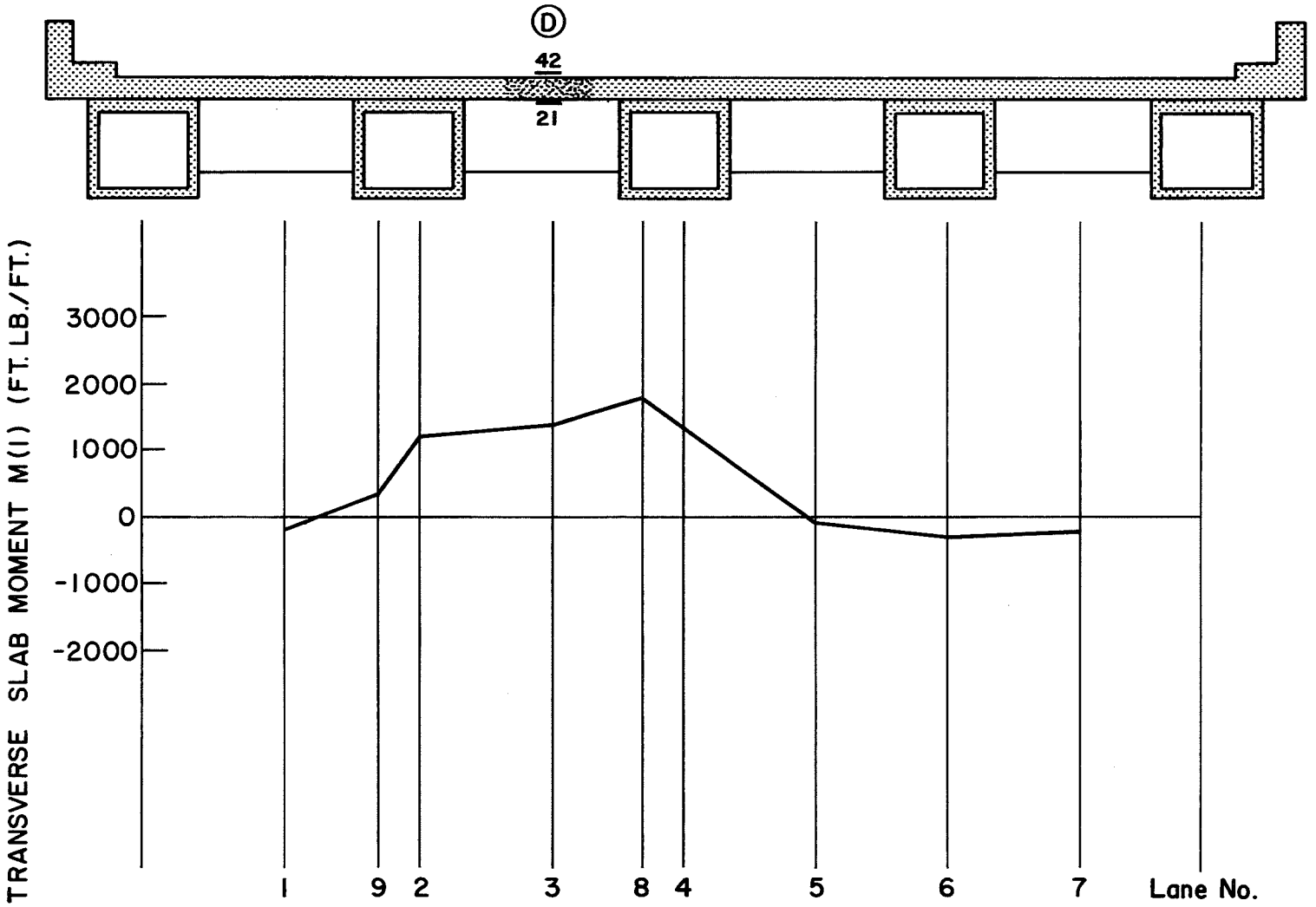

Fig. 32 Influence Lines for Transverse Slab Moments - Section D

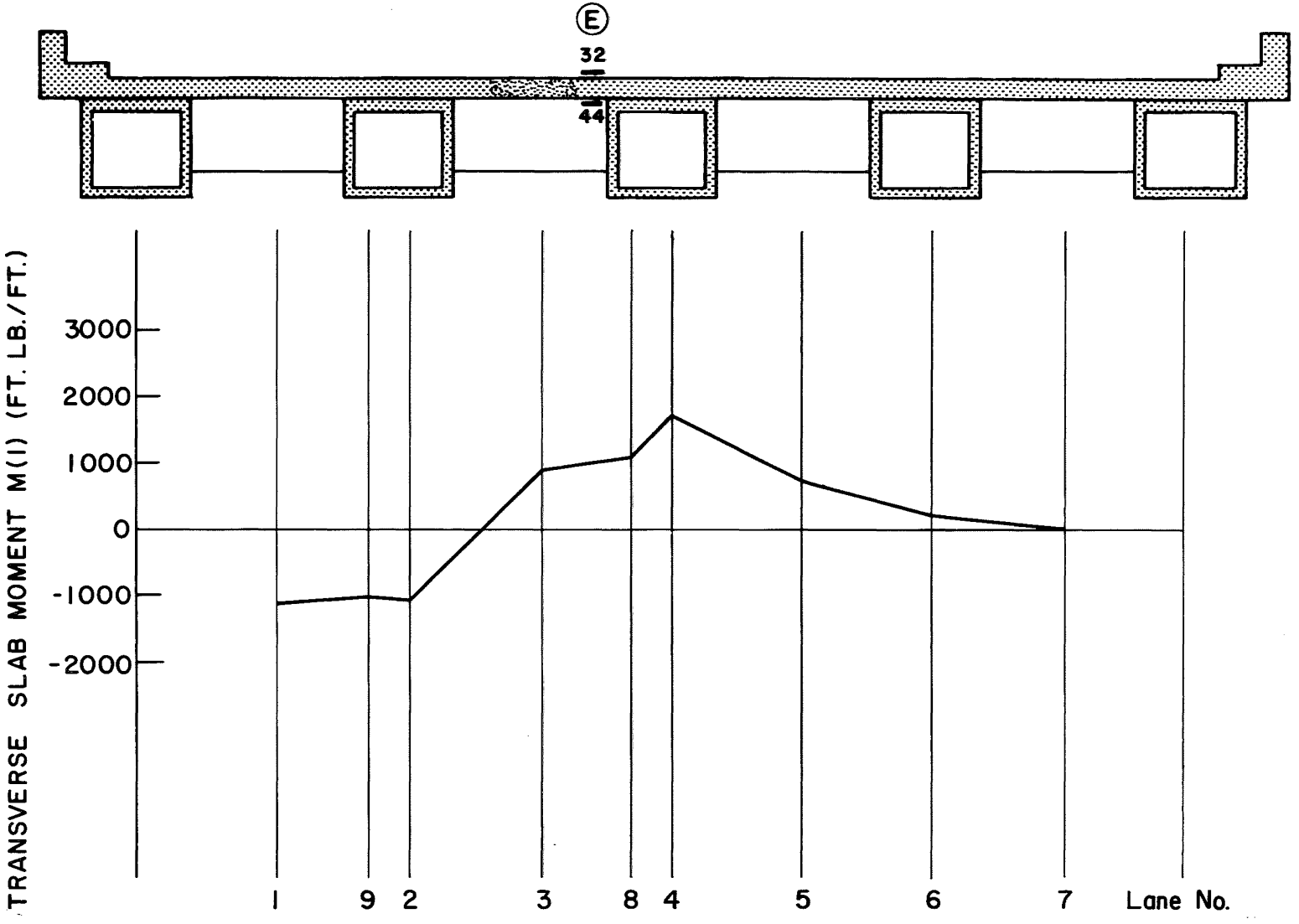

Fig. 33 Influence Lines for Transverse Slab Moments - Section E

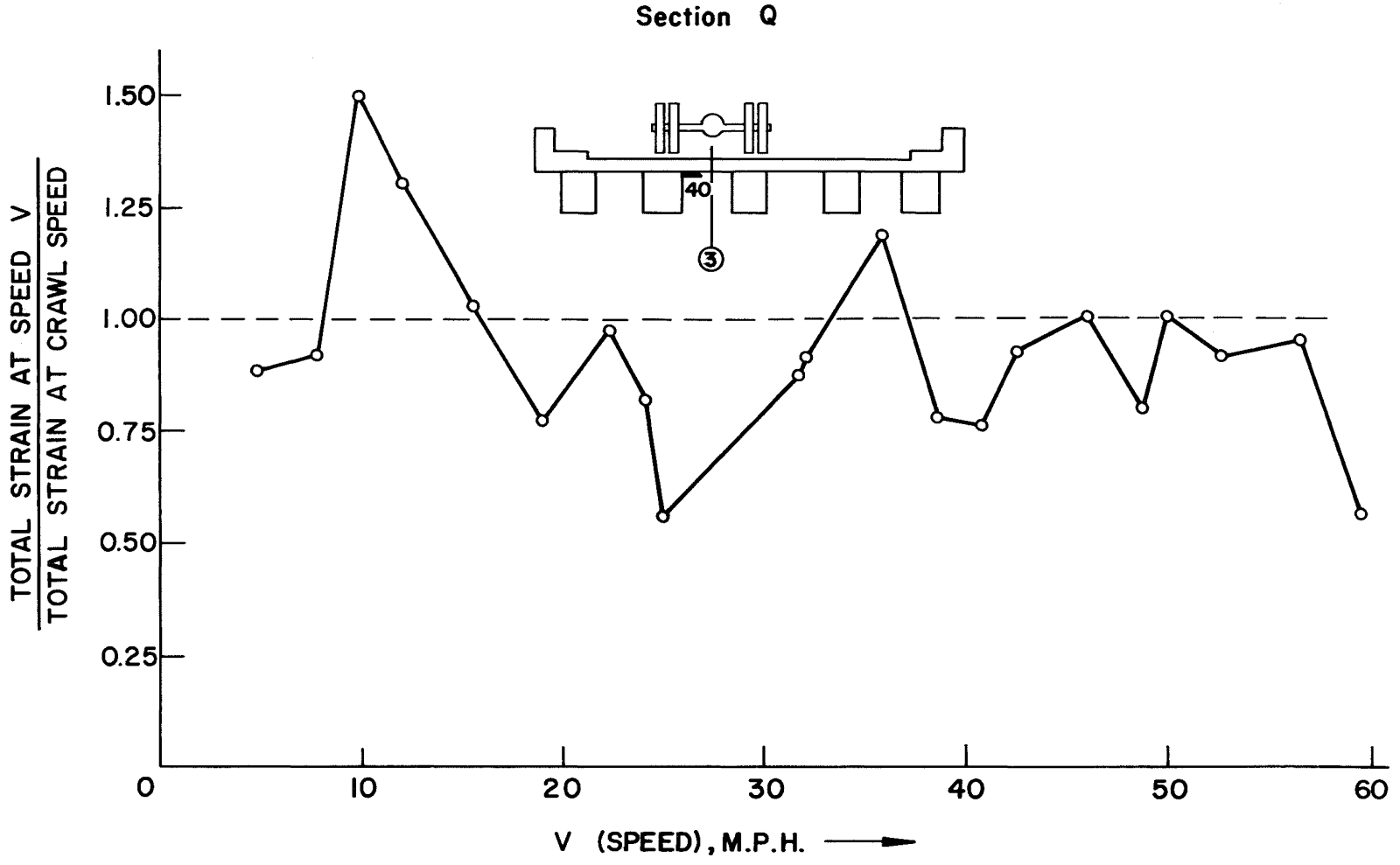

Fig. 34 Amplification Factor Versus Speed - Gage 40

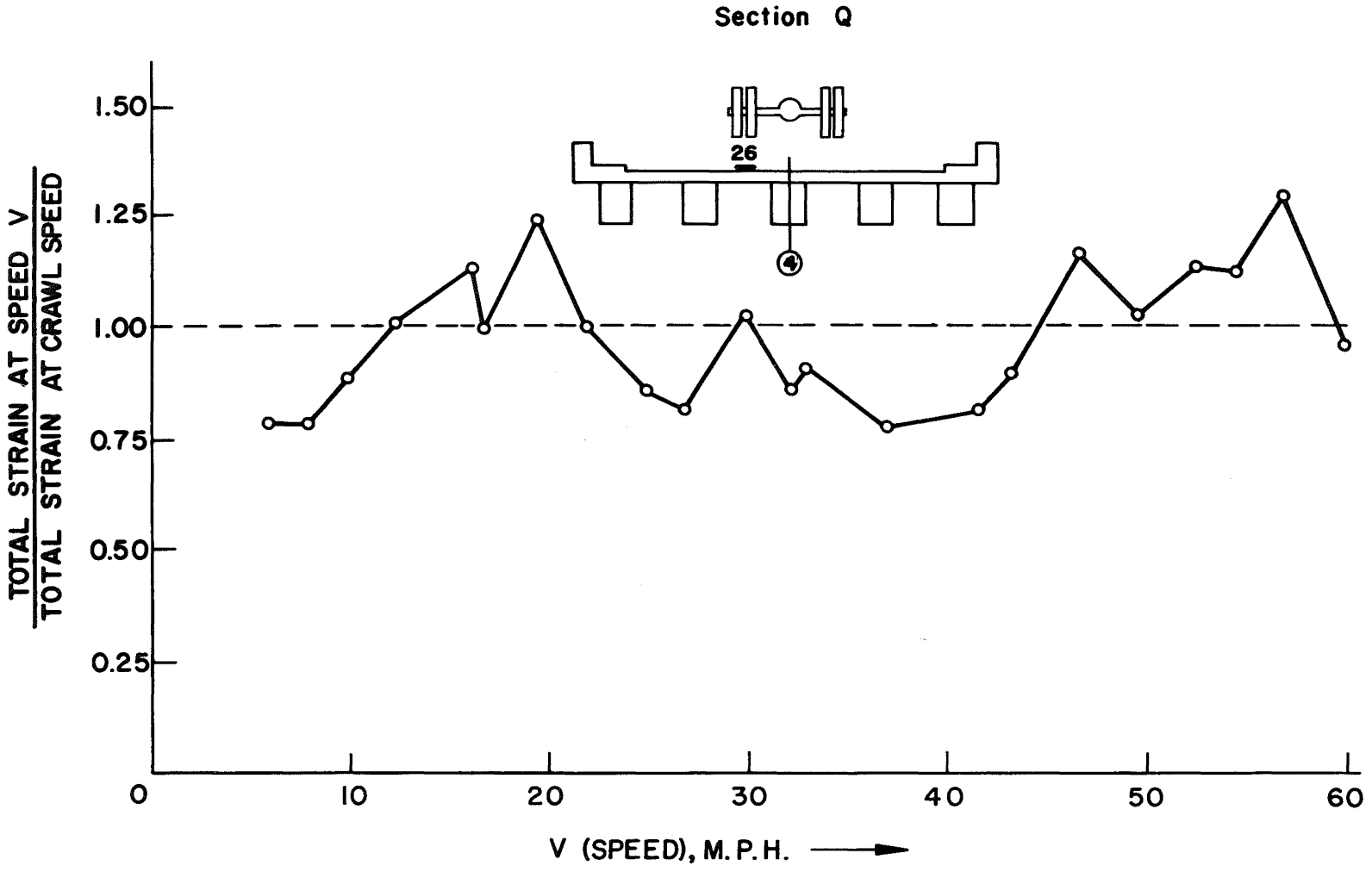

Fig. 35 Amplification Factor Versus Speed - Gage 26

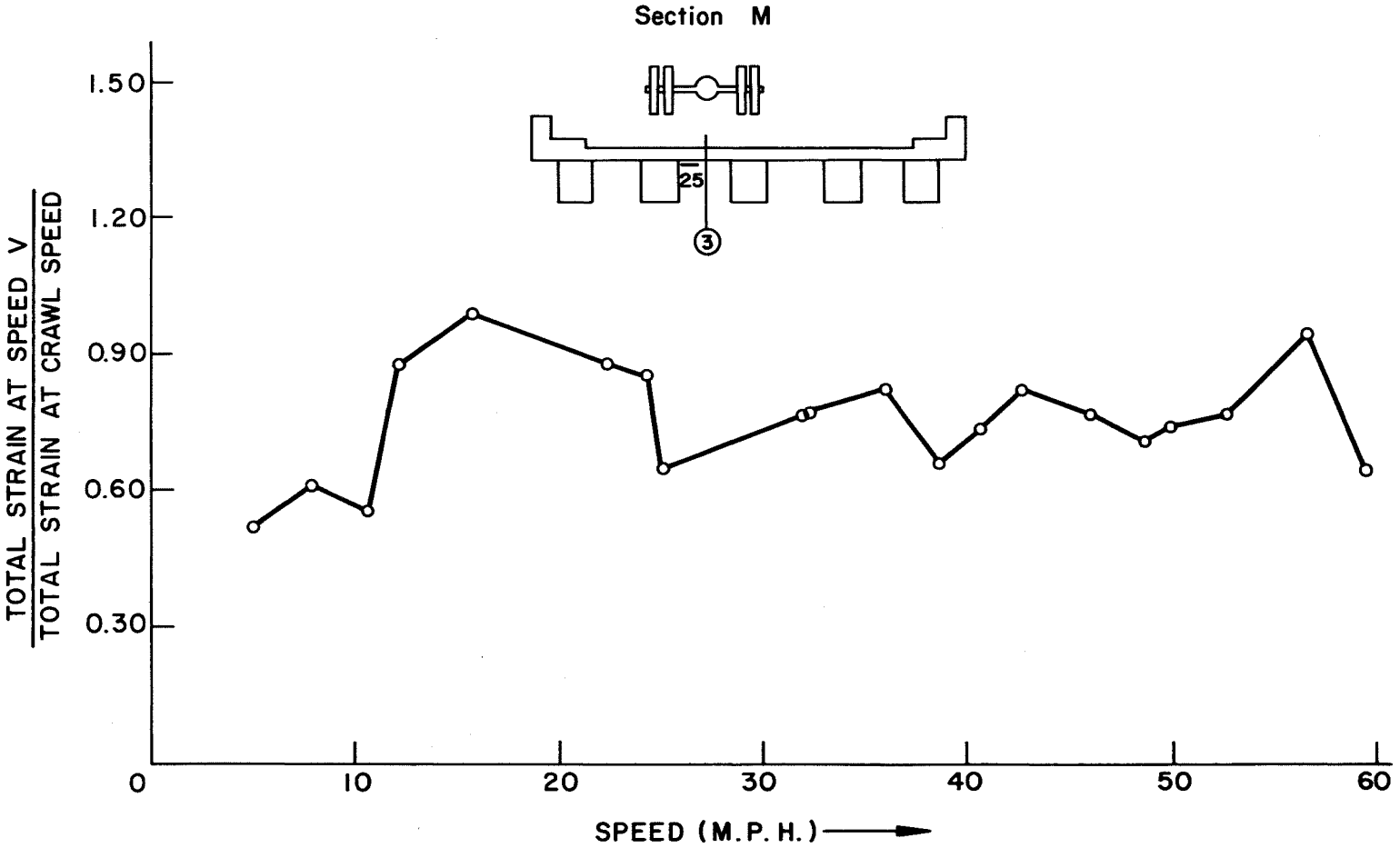

Fig. 36 Amplification Factor Versus Speed - Gage 25

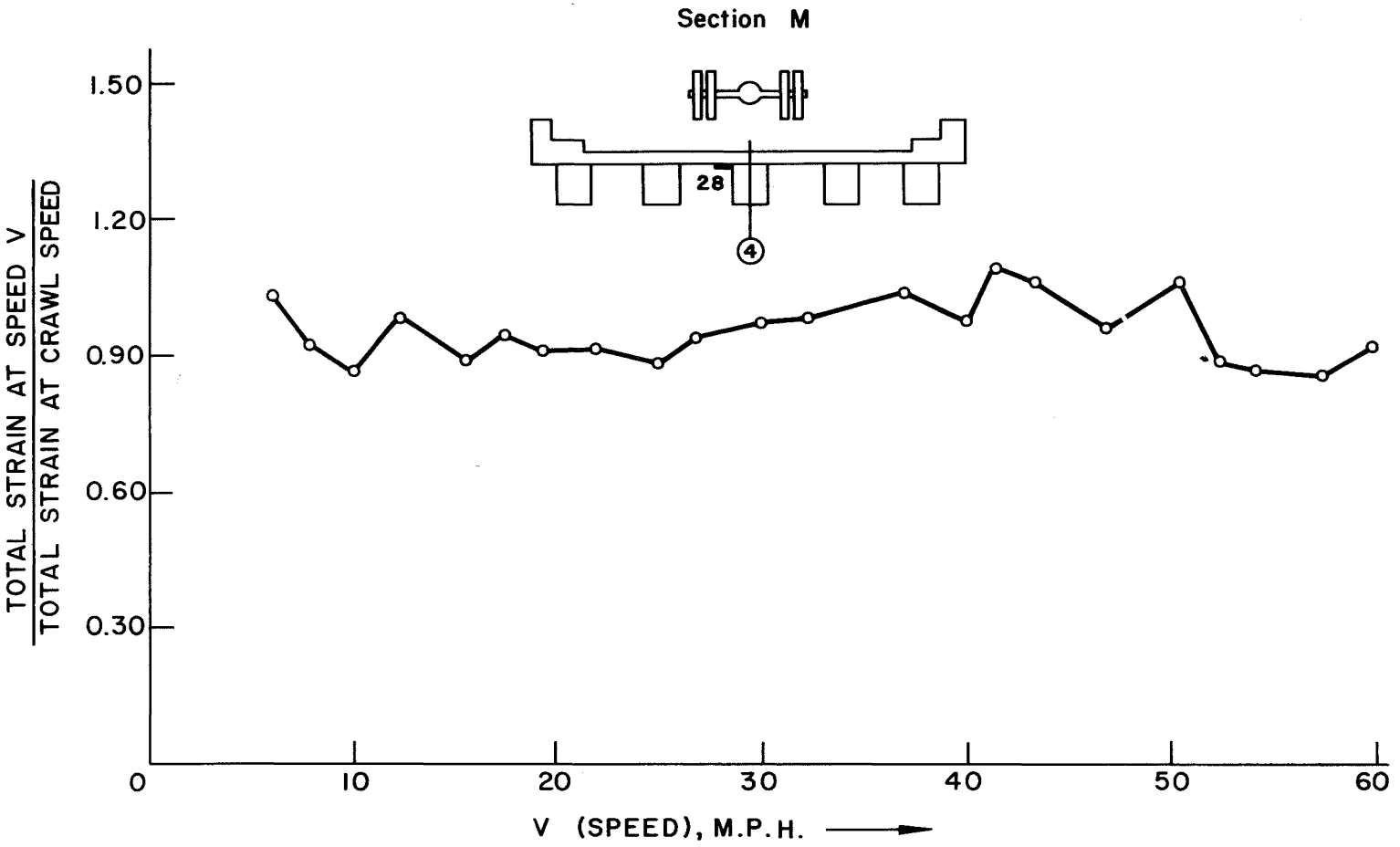

Fig. 37 Amplification Factor Versus Speed - Gage 28

10. REFERENCES

1. Timoshenko, S. P. and Goodier, J. N.
THEORY OF ELASTICITY, McGraw-Hill Book Company, Inc., New York, 1951.

2. American Association of State Highway Officials
STANDARD SPECIFICATIONS FOR HIGHWAY BRIDGES, Washington, D. C., 1969.

3. Reese, R. T.
A SUMMARY AND EXAMINATION OF EXISTING METHODS OF ANALYSIS AND DESIGN OF LOAD DISTRIBUTION IN HIGHWAY BRIDGE FLOORS, M.S. Thesis, Brigham Young University, 1966.

4. Guilford, A. A. and VanHorn, D. A.
LATERAL DISTRIBUTION OF DYNAMIC LOADS IN A PRESTRESSED CONCRETE BOX-BEAM BRIDGE, DREHERSVILLE BRIDGE, Fritz Engineering Laboratory Report No. 315.2, Lehigh University, 1967.

5. Guilford, A. A. and VanHorn, D. A.
LATERAL DISTRIBUTION OF VEHICULAR LOADS IN A PRESTRESSED CONCRETE BOX-BEAM BRIDGE, BERWICK BRIDGE, Fritz Engineering Laboratory Report No. 315.4, Lehigh University, 1967.

6. Schaffer, Thomas and VanHorn, D. A.
STRUCTURAL RESPONSE OF A 45° SKEW PRESTRESSED CONCRETE BOX-GIRDER HIGHWAY BRIDGE SUBJECTED TO VEHICULAR LOADING, BROOKVILLE BRIDGE, Fritz Engineering Laboratory Report No. 315.5, Lehigh University, 1967.

7. Guilford, A. A. and VanHorn, D. A.
LATERAL DISTRIBUTION OF VEHICULAR LOADS IN A PRESTRESSED CONCRETE BOX-BEAM BRIDGE, WHITE HAVEN BRIDGE, Fritz Engineering Laboratory Report No. 315.7, Lehigh University, 1968.

8. Lin, C. S. and VanHorn, D. A.
THE EFFECT OF MIDSPAN DIAPHRAGM ON LOAD DISTRIBUTION IN A PRESTRESSED CONCRETE BOX-BEAM, PHILADELPHIA BRIDGE, Fritz Engineering Laboratory Report No. 315.6, Lehigh University, 1968.

9. Newmark, N. M. and Siess, C. P.
RESEARCH ON HIGHWAY BRIDGE FLOORS, Highway Research Board Proceedings, 1954.

10. Erps, H. R., Googins, A. L. and Parker, J. L.
DISTRIBUTION OF WHEEL LOADS AND DESIGN OF REINFORCED CONCRETE BRIDGE FLOOR SLABS, Public Roads, October, 1937.

11. Newmark, N. M. and Siess, C. P.
MOMENTS IN I-BEAM BRIDGES, University of Illinois Engineering Experiment Station Bulletin No. 336, June, 1942.

12. Westergaard, H. M.
COMPUTATION OF STRESSES IN BRIDGE SLABS DUE TO WHEEL LOADS, Public Roads, March, 1930.

13. Rowe, R. E.
CONCRETE BRIDGE DESIGN, John Wiley and Sons, New York, 1962.

14. Kelley, E. F.
EFFECTIVE WIDTH OF CONCRETE BRIDGE SLABS SUPPORTING CONCENTRATED LOADS, Public Roads, March, 1926.

15. Chen, Yan-Liang and VanHorn, D. A.
STRUCTURAL BEHAVIOR OF A PRESTRESSED CONCRETE BOX-BEAM BRIDGE, HAZLETON BRIDGE, Fritz Engineering Laboratory Report No. 315A.1, Lehigh University, 1970.